Draft version July 21, 2020
Typeset using LaTeX default style in AASTeX62

HO Puppis: A Sub-Luminous Hot Star with IW-And Type Light Curve

Chien-De Lee,[1] Jia-Yu Ou,[1] Po-Chieh Yu,[1,2] Chow-Choong Ngeow,[1] Po-Chieh Huang,[1] Wing-Huen Ip,[1] Franz-Josef Hambsch,[3,4,5] Hyun-il Sung,[6] Jan van Roestel,[7] Richard Dekany,[8] Andrew J. Drake,[7] Matthew J. Graham,[7] Dmitry A. Duev,[7] Stephen Kaye,[8] Thomas Kupfer,[9] Russ R. Laher,[10] Frank J. Masci,[10] Przemek Mróz,[7] James D. Neill,[8] Reed Riddle,[8] Ben Rusholme,[10] and Richard Walters[8]

[1] *Graduate Institute of Astronomy, National Central University, Jhongli 32001, Taiwan*
[2] *College of General Studies, Yuan-Ze University, Chung-Li, Taiwan*
[3] *American Association of Variable Star Observers (AAVSO), Cambridge, MA, USA*
[4] *Vereniging Voor Sterrenkunde (VVS), Oostmeers 122 C, 8000 Brugge, Belgium*
[5] *Bundesdeutsche Arbeitsgemeinschaft fr Vernderliche Sterne e.V. (BAV), Munsterdamm 90, D-12169 Berlin, Germany*
[6] *Korea Astronomy and Space Science Institute (KASI), Bohyunsan Optical Astronomy Observatory (BOAO), Youngcheon, Gyungbuk 38812, Republic of Korea*
[7] *Division of Physics, Mathematics, and Astronomy, California Institute of Technology, Pasadena, CA 91125, USA*
[8] *Caltech Optical Observatories, California Institute of Technology, Pasadena, CA 91125, USA*
[9] *Kavli Institute for Theoretical Physics, University of California, Santa Barbara, CA 93106, USA*
[10] *IPAC, California Institute of Technology, Pasadena, CA 91125, USA*

Submitted to AJ

ABSTRACT

HO Puppis (HO Pup) was considered as a Be star candidate due to its γ Cassiopeiae-type light curve, but lacks spectroscopic confirmation. Using distance measured from Gaia Data Release 2 and the spectral energy distribution (SED) fitting on broadband photometry, the Be star nature of HO Pup is ruled out. In contrast, the SED of HO Pup can be fit well with a hot and sub-luminous star or, possibly, a hot subdwarf. Furthermore, based on the 28,700 photometric data points collected from various time-domain surveys and dedicated intensive monitoring observations, the light curves of HO Pup resemble well to the IW And-type stars, exhibiting characteristics such as standstill phase, outbursts and dip events. The light curves of HO Pup display various variability time scales, including outbursts cycles range from 23 to 61 days, variations with periods of 3.9 days and 50 minutes during the standstill phase, and a semi-regular $\sim$ 14 days for the dip events. We have also collected time-series spectra (with various spectral resolutions), at which Balmer emission lines and other expected spectral lines for an IW And-type star were detected, even though some of these lines were also expected to be present on Be stars. Nevertheless, detection of Bowen fluoresces near the outburst phase can be used to discriminate between IW And-type stars and Be stars. Finally, despite only observing for 4 nights, the polarization variation was detected, indicating that HO Pup has intrinsic polarization.

1. INTRODUCTION

Be phenomenon is the photometric and spectroscopic variability seen in the main-sequence luminous rapid rotators, known as Be stars, with a luminosity class III−V. In recent years, we have studied the evolutionary effect on the formation of Be stars in the open clusters using the Palomar Transient Factory (PTF) and the intermediate Palomar Transient Factory (iPTF) data (Yu et al. 2015, 2016, 2018). The Zwicky Transient Facility (ZTF, Bellm et al. 2019; Graham et al. 2019; Masci et al. 2019) came after iPTF, so we have the ability to extent our investigation on the variability of Be stars (Ngeow et al. 2019), especially for the Be stars and Be star candidates at the faint end ($m > 13$ mag) which were largely excluded in previous works (e.g., in Labadie-Bartz et al. 2017). Together with

Corresponding author: Chow-Choong Ngeow
cngeow@astro.ncu.edu.tw

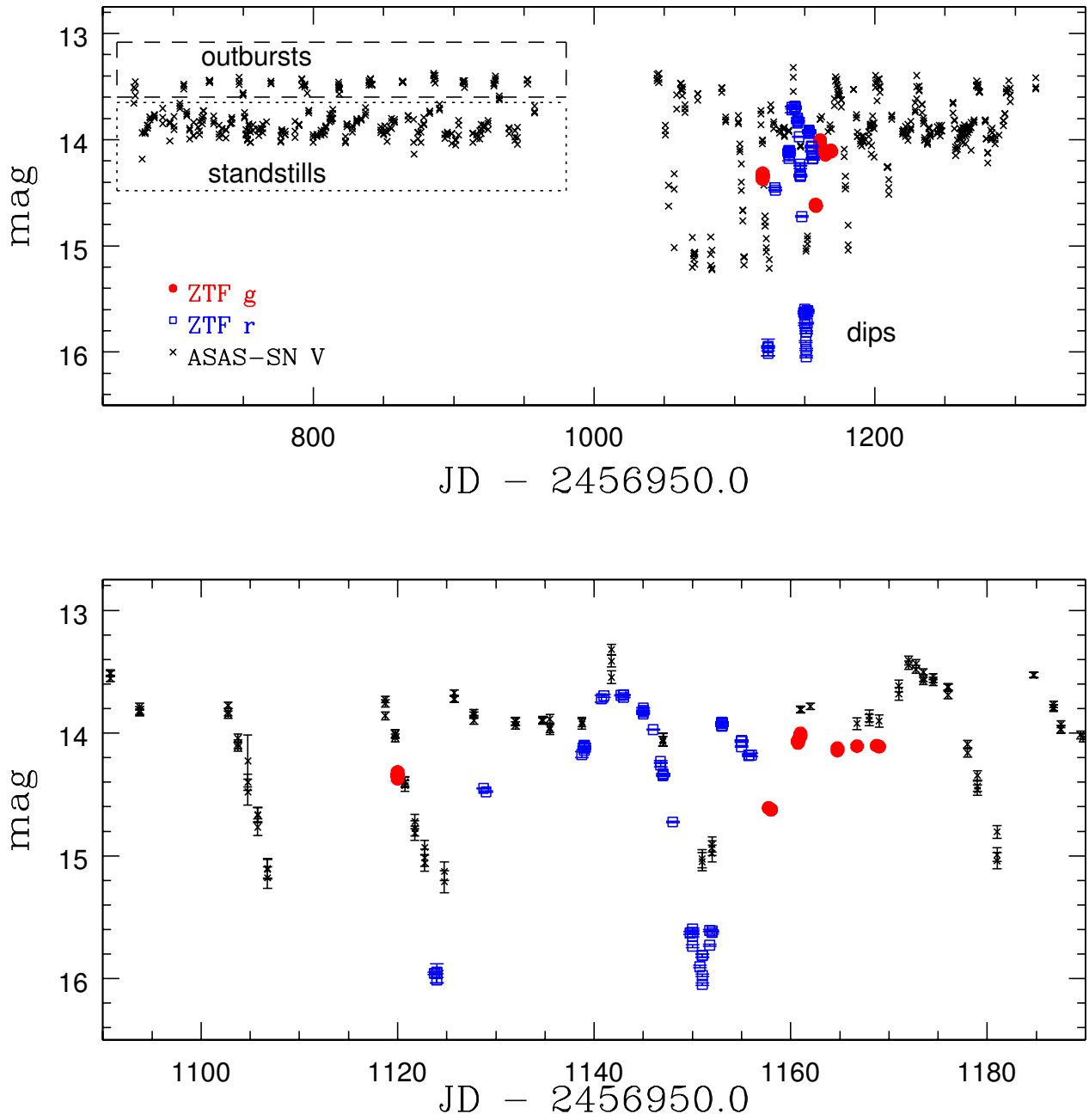

Figure 1. The ZTF g-band (red), r-band (blue) and ASAS-SN V-band (black) light curves of HO Pup. The top panel shows a portion of the light curve across $\sim$ 600 days, together with terminologies that would be used in this work to describe the light curve features: standstills (data points in the dotted box) are part of the light curves with magnitudes close to the mean value; outbursts are data points (in the dashed box) showing a brightening of $\sim$ 0.5 mag; and dips are events that fade by more than $\sim$ 1 mag from the mean magnitude. Several fading events with $\sim$ 2.5 mag dips were observed recently. This epoch with a number of deep dips events is zoomed in the bottom panel. Consistency of the light curves seen in both ZTF and ASAS-SN observations ruled out the possibility of such dips were due to instrumental effects.

accompanying time-series spectroscopic data, we have a new opportunity to explore the fundamental time-domain nature of Be stars.

Here we report the photometric characteristics of HO Puppis (HO Pup, $\alpha_{J2000} = 7^h33^m54\overset{s}{.}18$, $\delta_{J2000} = -15°45'38\overset{''}{.}28$) during our investigations of the Be stars variability with ZTF. HO Pup is listed as a Be star in the SIMBAD database (Manek 1997) and hence included in our list of Be star candidates, at which the classification was based on its γ Cassiopeia (GCAS) type variability recorded by Samus et al. (2017) – a class of variable stars that exhibit eruptive irregular variability which is not easy to be classified further. Some early literature even suggested HO Pup was a possible type Ia supernova with V-band photometry varying between 12.7 mag and 14.2 mag (Kukarkin et al. 1971). As presented in Figure 1, two highly unusual ~ 2.5 magnitude dips of HO Pup were observed by ZTF in 2017 November. In r-band, the ZTF data cover the full brightness minimum of the two dips at 16 mag from near the minimum to maximum brightness within two days because of the high cadence sampling. These two events were also witnessed by the All-Sky Automated Survey for Supernovae (ASAS-SN, Shappee et al. 2014; Kochanek et al. 2017) survey. In addition to these two events recorded by ZTF and ASAS-SN, we have found more dips based on literature and archival data since 2009 (see Section 2). These dips with amplitudes of ~ 2.5 mag are very unusual to be observed in typical Be stars, and hence HO Pup caught our attention and merit a further investigation.

The variability behavior of HO Pup was also considered as a special kind of cataclysmic variables (CV). The ASAS-SN light curve of HO Pup was discussed in a recent work by Kimura et al. (2020). In their study, HO Pup was classified as a dwarf nova (DN) with unique heartbeat-like oscillation in their photometric variation, known as IW And-type stars. Stars that display IW And-type phenomenon represents a new sub-classification of Z Cam stars (Kato 2019). The feature characteristics of IW And-type stars include eclipsing-like transits happen once in a while, in addition to repeated outburst/super-outburst seen in their light curves. Besides the prototypical object, IW And, there are only six additional DN being classified as IW And-type stars in the literature: IM Eri, FY Vul, V507 Cyg, ST Cha, NY Ser and V513 Cas (see Kimura et al. 2020, and reference therein). HO Pup could be an additional member of the IW And-type stars (Kimura et al. 2020).

Given the ambiguous nature of HO Pup, we collected its light curves data as much as possible from archival catalogs, some ongoing surveys and new dedicated observations. These collections of light curves were presented in Section 2. In addition to light curves data, we have also performed spectroscopic and polarimetric observations on HO Pup, described further in the same section. Analysis and results based on the data collected were presented in Section 3, at which we also presented the first emission line spectra of HO Pup – confirming its emission-line object nature. In Section 4, we will discuss the scenarios for the observed unusual light curves behaviours of HO Pup, followed by summaries of our work presented in Section 5.

2. OBSERVATIONS AND DATA

Time-series photometric data ranging from optical to infrared for HO Pup were collected from various survey catalogs. These includes: the ZTF, the ASAS-SN, the Digital Access to a Sky Century @ Harvard (DASCH), the third phase of the All Sky Automated Survey (ASAS-3), the Panoramic Survey Telescope and Rapid Response System 3π survey (Pan-STARRS), the Wide-field Infrared Survey Explorer (WISE), and observations available via the American Association of Variable Star Observers (AAVSO). These light curves data were supplemented with dedicated observations taken at the Lulin Observatory. All of these light curves were merged in Figure 2, and listed in Table 1, that covering form 1894 to 2020. We also summarized these light curves data in Table 2. Following the terminologies use to describe the light curves of IW And-type stars (Kimura et al. 2020), definitions of main features exhibited in the light curves, such as dips, outbursts and standstills, were demonstrated in the upper panel of Figure 1. For spectroscopic observations, we have spectra collected from P60/SEDM, BOAO/BOES, CFHT/EsPADOnS and P200/DBSP. Additionally, polarization was measured in four different nights using the TRIPOL2 instrument at the Lulin Observatory in late-October 2018.

2.1. *Optical and Infrared Light Curve Data*

ZTF is an northern sky synoptic survey project ($\delta > -30°$) carried out by the 1.2-m Samuel Oschin telescope at the Palomar Observatory. With a superb large field-of-view mosaic CCD camera (47deg^2 with 1.0″ pixel scale), the Galactic plane can be scanned once a night with g and/or r filter. For HO Pup, 54 and 494 good quality measurements were taken in g- and r-band, respectively, between 2017 December and 2018 December.

ASAS-SN data are taken by couple quadruple telescopes located in both hemispheres. The mounted cameras have a 4.5deg^2 field of view with a pixel scale of 7.8″. This survey provides us the longest time baseline from 2012 to 2020 containing 960 V-band and 937 g-band measurements.

AAVSO responded quickly to involve the monitoring of HO Pup with V-band, right after our report of this extraordinary event to the ZTF community. In 2018 October 13, AAVSO started to collect data with extremely well coverage

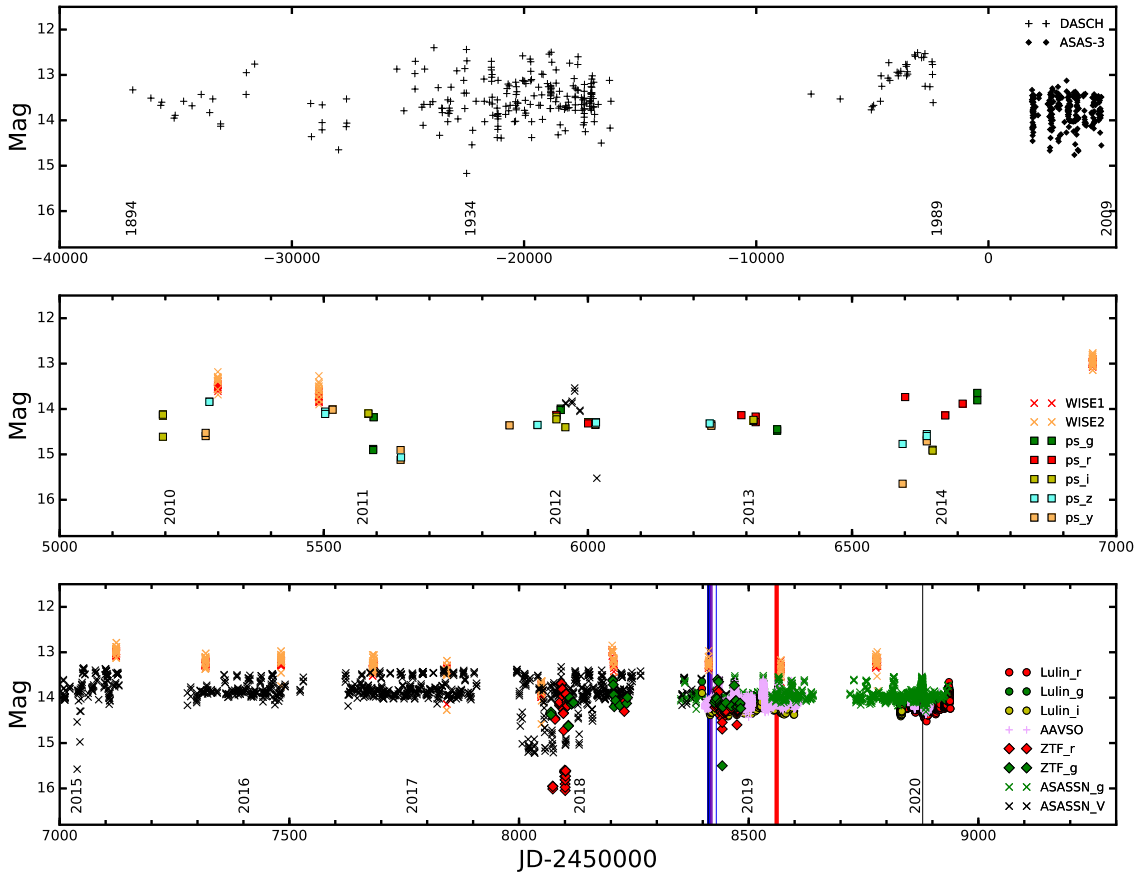

Figure 2. The light curve of HO Pup across more than a century from optical to mid-infrared consisting of AAVSO, ASAS-3, ASAS-SN, DASCH, Lulin (with SLT), Pan-STARRS (PS), WISE and ZTF. Each data points (for clarity, error bars are ignored) is noted with data source and filters accordingly. The observation time of followup spectroscopic and polarimetric observations are marked with vertical lines containing P60/SEDM (blue), LOT/TRIPOL2 (purple), BOAO/BOES (black line in 2018), CFHT/ESPanDOnS (red) and P200/DBSP (black line in 2020). More details can be seen in upper panel of Figure 3 and Figure 4 with a zoom-in on the individual duration.

in time domain, using a ML16803 CCD camera with a pixel scale of 2.06″ equipped on a 0.4-m telescope at the Remote Observatory Atacama Desert (ROAD, Hambsch 2012) in San Pedro de Atacama, Chile. Every clear night, ROAD monitored HO Pup more than 5 hours with about 50 measurements, resulting a total of 10890 photometric data points. The typical uncertainty on this set of photometry is about 0.02 mag, and we use a 0.15 mag cut as our quality cut after testing several values.

Pan-STARRS used five filters[1], g_{p1}, r_{p1}, i_{p1}, z_{p1} and y_{p1}, to survey the sky. It has a wide-field 7deg^2 mosaic camera with a pixel scale of 0.26″, equipped on the dedicated 1.8-m Pan-STARRS telescope which is located at the Haleakala Observatory in Hawaii (Kaiser et al. 2010; Chambers et al. 2016). HO Pup were observed over a full four years time span (2009-2015). In contrast to ASAS-SN or AAVSO, there is only a limited amount of observations (numbers) were taken. Two significant dips (m >15.5 mag) were also recorded by Pan-STARRS.

The 0.4-m SLT telescope, located at the Lulin Observatory in Taiwan, was used to perform near simultaneous gri-band and intensive r-band monitoring follow-up observations of HO Pup. Together with the equipped Apogee

[1] For simplicity, we referred them as g, r, i, z and y in the rest of this paper.

Table 1. Collected light curves with 28700 data points for HO Pup.

MJD	Mag	Uncertainty	Band	Source
13146.3190	13.330	0.100	*B*	*DASCH*
13929.2218	13.510	0.170	*B*	*DASCH*
14353.0697	13.670	0.170	*B*	*DASCH*
14393.0297	13.600	0.170	*B*	*DASCH*
14927.3884	13.950	0.120	*B*	*DASCH*
14972.2725	13.890	0.160	*B*	*DASCH*
15336.3097	13.580	0.150	*B*	*DASCH*
15697.3473	13.680	0.150	*B*	*DASCH*
16093.2480	13.430	0.090	*B*	*DASCH*
16458.2944	13.830	0.180	*B*	*DASCH*
...	...	...	...	...

Note—The entire Table will be available in its electronic form at the `SIMBAD` archive.

Table 2. Summary of light curves data.

Band	Database	N	MJD_{start}	MJD_{end}	UT $Date_{start}$	UT $Date_{end}$	Mean Mag.	Std.
B	DASCH	260	13146.3	47616.4	11-14-1894	03-31-1989	13.472	0.463
g	ZTF	54	58107.4	58482.5	12-20-2017	12-30-2018	14.136	0.288
g	ASAS-SN	937	58220.2	58933.2	04-12-2018	03-25-2020	13.954	0.130
g	Lulin/SLT	313	58397.9	58832.7	10-06-2018	12-15-2019	14.128	0.089
g	Pan-STARRS	12	55593.4	56737.3	02-01-2011	03-21-2014	14.261	0.382
V	ASAS-3	217	51874.2	54862.2	11-26-2000	01-31-2009	13.793	0.310
V	ASAS-SN	960	55957.4	58450.6	01-31-2012	11-28-2018	13.860	0.324
V	AAVSO	10890	58404.3	58915.2	10-13-2018	03-07-2020	14.094	0.134
r	ZTF	494	58073.3	58476.4	11-16-2017	12-24-2018	14.283	0.311
r	Lulin/SLT	13786	58397.9	58938.6	10-06-2018	03-30-2020	14.190	0.099
r	Pan-STARRS	10	55940.4	56709.3	01-14-2012	02-21-2014	14.109	0.175
i	Lulin/SLT	309	58397.9	58832.7	10-06-2018	12-15-2019	14.293	0.067
i	Pan-STARRS	13	55195.4	56652.5	12-30-2009	12-26-2013	14.332	0.292
z	Pan-STARRS	14	55283.3	56641.5	03-28-2010	12-15-2013	13.311	0.336
y	Pan-STARRS	15	55276.2	56641.5	03-21-2010	12-15-2013	14.327	0.423
W1	WISE	208	55298.7	58780.5	04-12-2010	10-24-2019	13.338	0.249
W2	WISE	208	55298.7	58780.5	04-12-2010	10-24-2019	13.280	0.273

U42 CCD, SLT has a pixel scale of 0.79″. We used 77 reference stars located within 0.5° from HO Pup to perform differential photometry and calibrated to the Pan-STARRS catalog. The SLT data provides a significant support on variability investigation in short time scale and monitoring the color variation in optical as the multi-band data from the optical surveys mentioned earlier were not taken simultaneously or near simultaneous (hence no color information).

WISE is an all-sky survey mission that mapped the entire sky at 3.4, 4.6, 12, and 22 μm (hereafter called as W1, W2, W3, and W4) with spatial resolutions of 6.1″ and 6.4″ in W1 and W2 bands (Mainzer et al. 2011). The near-earth object WISE (NEOWISE) project is particularly designed to hunt for asteroids using the W1 and W2 bands, and it provides infrared (IR) data over nine years from 2010 April to 2019 October. The cadence of the WISE observations is about twice a year; each observation includes about a dozen of measurements over one day.

Finally, we included the DASCH and ASAS-3 light curves data, but they were not used in subsequent analysis. The DASCH project (Grindlay et al. 2012) have digitized photometric measurements from nearly 500,000 glass plates

across 100 years. With a quality cut of 0.2 mag, 260 Johnson B-band magnitudes were selected for HO Pup from 1894 up to 1989 as historical records. One possible dip is included (see subsection 3.2). In case of ASAS-3 data (Pojmanski 1997, 2002), we excluded them in the analysis because of the associated large pixel scale ($\sim 15''$). Therefore issue of blending is unavoidable at the location of HO Pup. Nevertheless, we extracted 217 V-band light curve data (grade A and B only) from the ASAS-3 archive. These light curve data were measured using the smallest ASAS-3 aperture size (Pojmanski et al. 2005, 2 pixels; corresponding to the `MAG_0` in ASAS-3 catalogs).

2.2. *Spectroscopic Data*

Soon after the 2.5 mag dips found by ZTF in late 2017, we have collected spectra of HO Pup based on the observations carried out in 2018 by P60/SEDM and BOAO/BOES, in 2019 by CFHT/ESPaNDOnS, as well as in 2020 by P200/DBSP. Due to the nature of queue observation of these telescopes and instruments, none of the spectra were taken during the 2.5 mag dip event of HO Pop, which did not occur again after mid-2018.

The Spectral Energy Distribution Machine (SEDM, Ben-Ami et al. 2012; Ritter et al. 2014; Blagorodnova et al. 2018; Rigault et al. 2019) is a low-resolution IFU (integral field unit) spectrograph, mounted on the robotic P60 telescope at the Palomar Observatory (Cenko et al. 2006), providing efficient follow-up observations. The dispersion on the red side and blue side are 35 and 17.4 Å per pixel, respectively. Queued observations of SEDM were carried out multiple times between 2018 October 19 and 2018 November 07, but only spectra from four nights were usable. The data were automatically reduced using the dedicated SEDM reduction pipeline (Rigault et al. 2019). As seen in Figure 3, the emission-like bump peaks in 6563 Å (indicated by a vertical dashed line) can be seen in all of the four spectra taken by SEDM.

We have also obtained an optical spectrum of HO Pup using the Bohyunsan Optical Echelle Spectrograph (BOES, Kim et al. 2002) in long-slit mode, equipped on the 1.8-m Optical Telescope at the Bohyunsan Optical Astronomy Observatory (BOAO) in South Korea, on 2018 October 20. The observation was conducted using the grating 300V with $3''$ slit width under $1.8''$ seeing, resulting a spectral resolution of ∼1200 Å. The coverage of wavelength is 3500–7000 Å and the exposure time is 40 minutes. We follow the standard procedures of data reduction using IRAF[2], e.g., flat-fielding, wavelength calibration with FeNeArHe lamp, and flux calibration with the standard star G191-B2B. The spectrum is shown in bottom panel of Figure 3. The Hα emission line is clearly detected with an equivalent width (EW) ~ -4.5 Å, estimated using the Astrolib PySynphot package (STScI Development Team 2013). Due to low signal-to-noise ratio below 5000$\AA$ of this spectrum, we cannot confirm the detailed spectral type of HO Pup.

To further investigate the Hα emission variability, we took high-resolution echelle spectra of HO Pup using the ESPaDOnS (Echelle SpectroPolarimetric Device for the Observation of Stars) mounted on the 3.6-m Canada-France-Hawaii Telescope (CFHT), with a spectral resolution of $R \sim 68{,}000$. The wavelength coverage is 3750−10400 Å at approximately 0.007Å/pixel, containing 40 grating orders. With exposure time of 2400s for spectroscopy (sky+star mode) and 4800s for spectropolarimetry (both were arranged by the CFHT queue observers), HO Pup was nightly observed from 2019 March 15 to 2019 March 22 under good seeing ($\lesssim 1''$) conditions. CFHT provided the user a set of fully reduced spectra from Libre Esprit, an automatic ESPaDOnS reduction package/pipeline (Donati et al. 1997, 2007). One of the brightening or outburst event from 14.1 mag to 13.6 mag was fortunately well observed in these eight nights. As shown in Figure 4, all Hα emission lines were clearly seen, despite that the parts of the continuum are barely observed.

Finally, a single 600 second spectrum was obtained using the Palomar 200-inch Telescope (P200) and the Double-Beam Spectrograph (DBSP, Oke & Gunn 1982) on 2020 January 30. A 2 arcsecond slit was used with the 600/4000 grating in the blue arm and the 316/7500 grating in the red arm, providing $R \sim 1500$. A wavelength calibration spectrum was taken directly after the science spectrum. A spectrum of a flux-standard star was obtained at the beginning and end of the night. The data were reduced using the pipeline developed by Bellm & Sesar (2016)[3]. Using the pipeline, we performed the standard bias corrections, flat field corrections, wavelength calibration and flux-calibration. We also automatically combined the red and blue spectra using this pipeline. The reduced spectrum is displayed in the lower panel of Figure 5, at which the Hα EW value is ~ -4.3 Å, also estimated using the Astrolib PySynphot package.

[2] IRAF is distributed by the National Optical Astronomy Observatory, which is operated by the Association of Universities for Research in Astronomy, Inc., under cooperative agreement with the National Science Foundation.

[3] https://github.com/ebellm/pyraf-dbsp

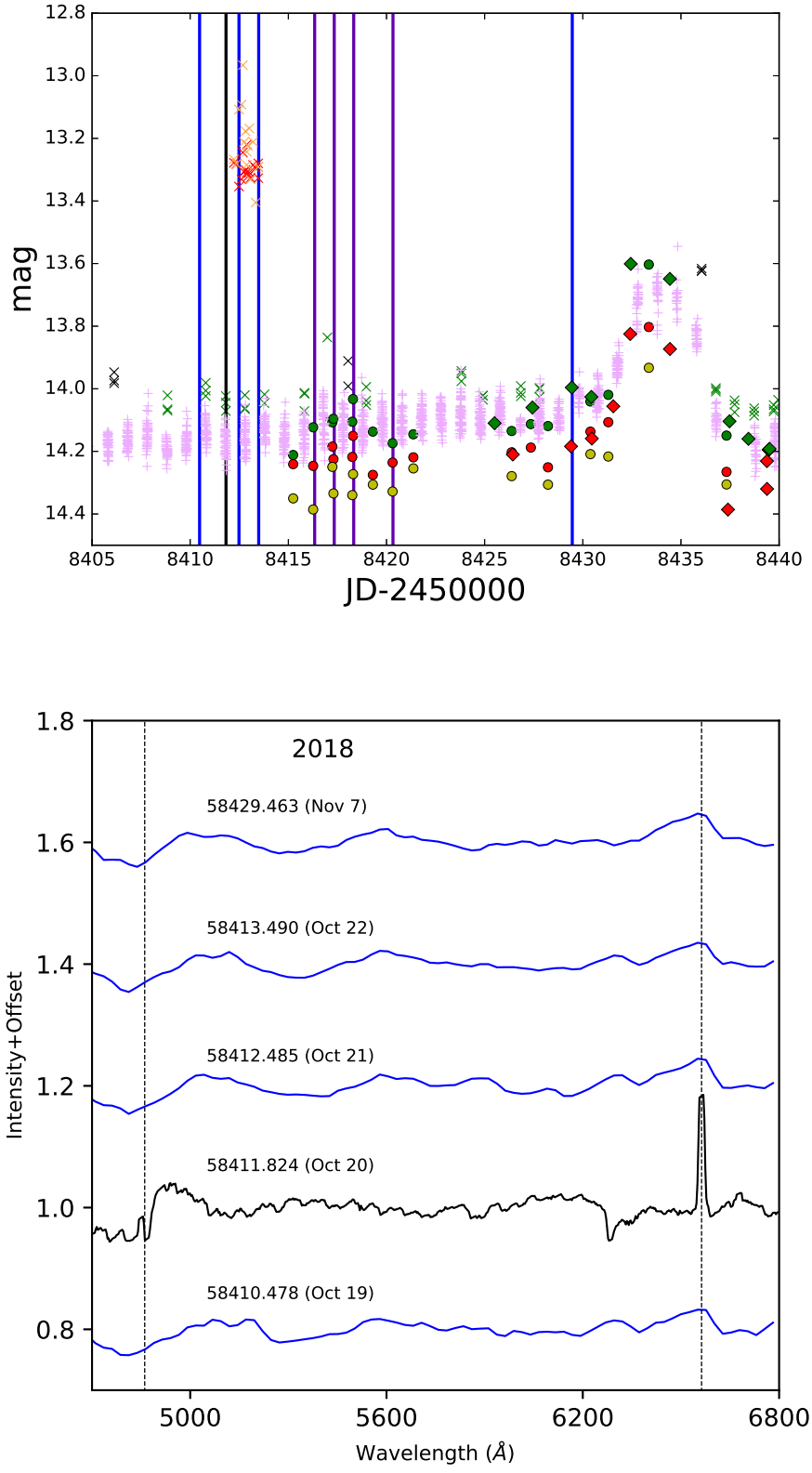

Figure 3. The top panel is same as Figure 2 but for the epoch with P60/SEDM (blue), BOAO/BOES (black) and LOT/TRIPOL2 (purple, see Table 3) observations. The bottom panel shows the P60/SEDM spectra (blue color) and BOAO/BOES spectrum (black color) resulted from a normalization using a 5^{th} order polynomial. Both of the Hα and Hβ lines (indicated by the dashed lines) are obviously seen in these spectra with either low or medium resolution, hence the emission nature of HO Pup was essentially confirmed. Previously, HO Pup is considered as a Be star candidate based on its classification as a GCAS type variable star.

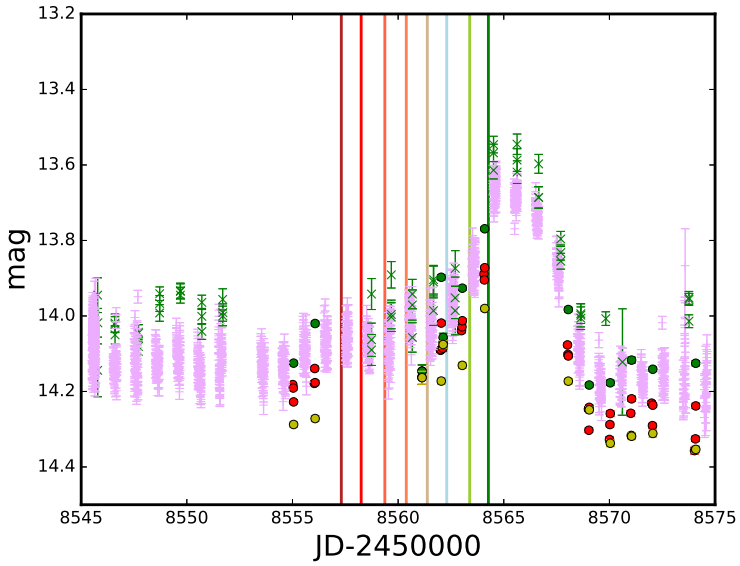

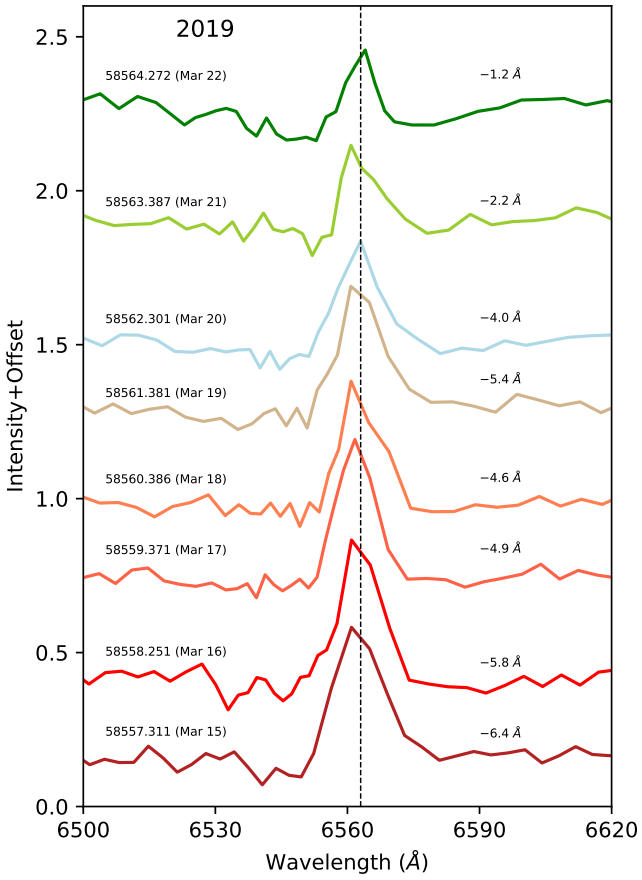

Figure 4. The top panel is same as Figure 2 but for the epoch with CFHT/EsPADOnS observations. The bottom panel shows the CFHT/EsPADOnS spectra of HO Pup taken from 2019 March 15 to 22, centered on Hα line. To improve the signal-to-noise ratio in the plot, the spectra were re-binned with a resolution of $\delta\lambda \sim 3$Å. Values on the right of each spectra are the measured EW of the Hα line, derived using the Astrolib PySynphot package (STScI Development Team 2013).

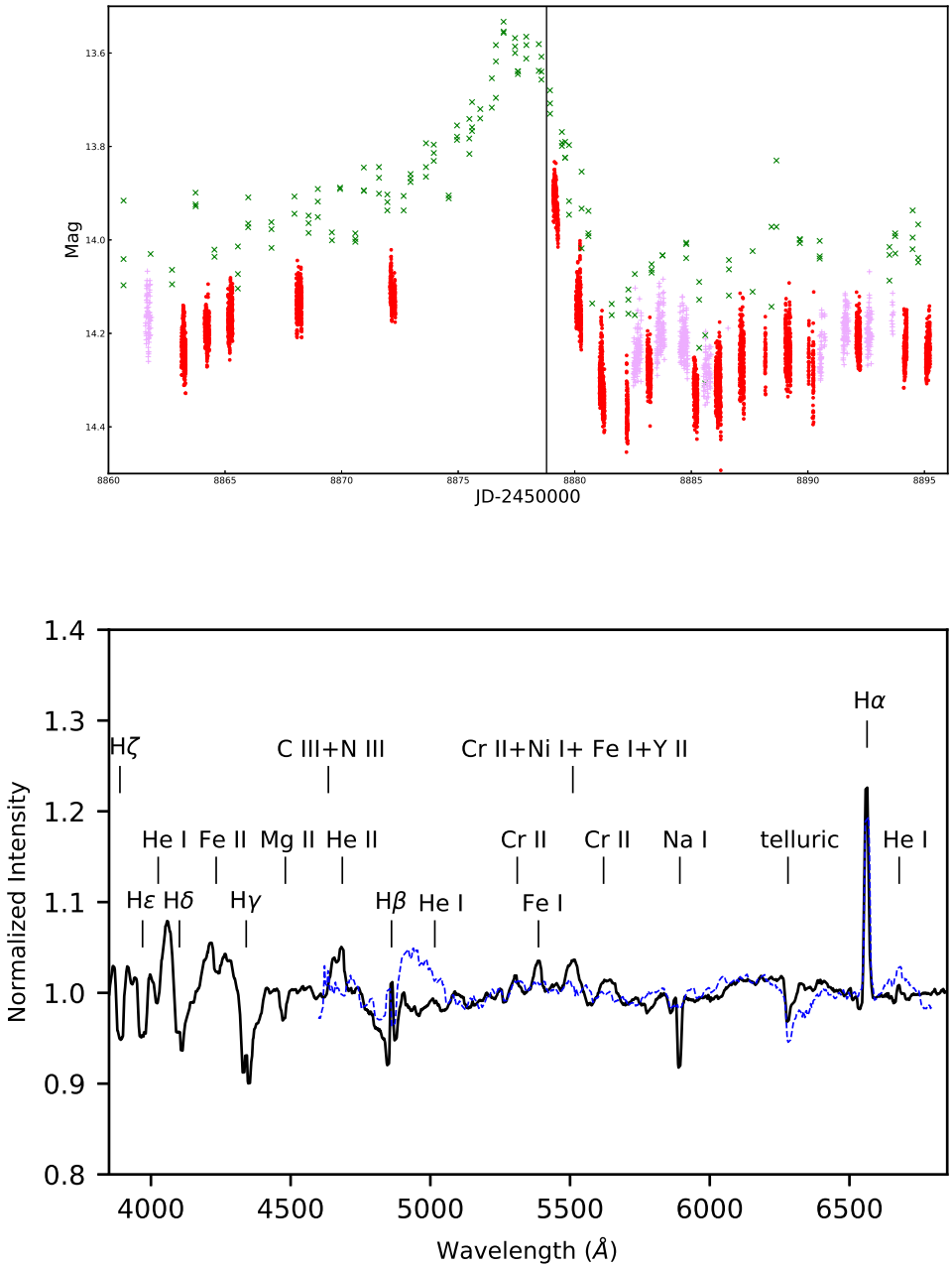

Figure 5. The top panel is same as Figure 2 but for the epoch with P200/DBSP spectroscopic observation (indicated by the vertical solid line), taken right after the photometric outburst maximum. This spectrum was shown in the bottom panel as a solid curve. For comparison, BOAO/BOES spectrum was over-plotted together as a (blue) dashed curve. The spectral characteristics of HO Pup, include hydrogen Balmer lines, as well as helium, iron, nickel, sodium and chromium lines, are identified.

2.3. *Polarimetric Data*

In addition to photometric and spectropic observations, we have also take the polarimetric data by using the TRIPOL2 (second generation of the Triple Range Imager and POLarimeter) instrument (Sato et al. 2019), equipped on the Lulin One-meter Telescope (LOT), in 2018 October. TRIPOL2 can take simultaneously polarization images in Sloan g'-, r'- and i'-band with half-wave plate rotating to four angles: 0°, 45°, 22°.5, and 67°.5. We measured the flux at each angles using aperture photometry following standard reduction procedures, and the Stokes parameters (I, Q

Table 3. Polarization values of HO Pup

Date	P_r (%)	θ_r (°)	P_i (%)	θ_i (°)
2018 October 24	0.7 ± 0.5	44.4 ± 22.5	0.9 ± 0.2	45.8 ± 34.1
2018 October 25	0.5 ± 0.5	135.8 ± 28.6	0.5 ± 0.5	132.9 ± 28.6
2018 October 26	1.5 ± 0.2	28.1 ± 11.3	0.8 ± 0.3	30.8 ± 42.4
2018 October 28	0.0 ± 0.5	25.6 ± 28.6	0.7 ± 0.7	128.3 ± 28.6

and U) were then derived. The polarization percentage $P = \sqrt{Q^2 + U^2}/I$ and the position angle $\theta = 0.5 \arctan(U/Q)$ can be calculated from these Stokes parameters with a typical accuracy of $\Delta P \lesssim 0.3\%$. Polarimetric data of HO Pup was well obtained in r- and i- bands (but it was too faint in the g-band), as reported in Table 3. We have also observed a number of unpolarized and polarized standard stars (Schmidt et al. 1992) to calibrate the instrumental polarization and angle offset (Sato et al. 2019). Based on the observations of these standard stars, we found that the performance of TRIPOL2 was very stable within those nights for both of the measurements of polarization percentages (using both polarized and unpolarized standard stars) and the polarization position angles (using the unpolarized standard stars); for more details, see Huang (2019). To reduce the influence by sky conditions, we also require that each of these four measurements has at least five sets of images with nearly the same count in each angles. This ensures us the polarization measurements are reliable from our nightly observations.

3. RESULTS

3.1. *An Emission-Line Object*

As mentioned in Introduction, HO Pup could be considered as a Be star candidate or a IW And-type DN, without any emission-line or even spectral observations reported in the literature. With our spectroscopic follow-up observations, the Hα emission line is clearly seen in each of our observations including the spectra from P60/SEDM, BOAO/BOES, CFHT/EsPADOnS and P200/DBSP (as shown in Figure 3, 4 and 5). Since the Hα emission EW is weak, e.g. $\sim -4.5\AA$ as measured in BOAO/BOES spectrum, the scarcely seen emission feature is expected in the low resolution spectra taken from P60/SEDM. Therefore, in addition to the known GCAS or IW-And type light curve variation, HO Pup is now confirmed as an emission-line object.

Beyond Hα, other prominent hydrogen, helium, and metal features can be easily identified. During the outburst phase, firstly, HO Pup obviously shows that Balmer lines, from Hβ to Hζ, are superposed on weak emission lines (see Figure 5). Secondly, the helium features were revealed including absorption lines He I 4026 Å and 4471 Å, and emission lines He I 5016 Å, 6678 Å and He II4713 Å. Thirdly, several metal absorption features can be identified, such as Fe II 4233 Å, Mg II4481 Å, Na I doublet 5889 Å and 5893 Å; other emission features include Cr II 5311 Å and 5620 Å, and Fe II 5387 Å. We also identified few blended emission lines such as C III+N III 4634-4651 Å (blended Bowen lines) and Cr II+Ni I+Fe I+Y II 5510 Å. Note that the spectral characteristics and EW variation of Hα emission for HO Pup will be discussed further in Section 4.

3.2. *The Dip Events*

Two 2.5-mag dips were observed by ZTF r- and g-band (13.5-16 mag; see Figure 1) in late 2017. During these significant events, ASAS-SN also witnessed these two dips in V-band. These dips observed in both independent surveys were well matched in the time sequence. When examining the long term light curve taken from ASAS-SN, in total there are eight dip events found between 2017 September to 2018 January, labelled as E1 to E8 in Table 4. Note that the dip event E4 was barely observed by ASAS-SN on 2017 October 23 (JD=2458049.806). Within half a day, WISE happened to catch the IR counterpart of the same event down to 14.58 mag in W2 band (JD=2458049.435). Just like other dips in optical band, the IR brightness drops significantly at this event when compared to the average brightness in WISE W2 band (13.280 mag).

These E1-E8 dips have almost the same shape, especially for the part on decreasing slopes. In Figure 6, we over plotted these events all-together, at which the very similar shapes of these dip events can be seen. Note that only the E6 and E7 dip events were found to drop by $\sim$ 2.5-mag, other events the drop in magnitudes range from $\sim$ 1 to

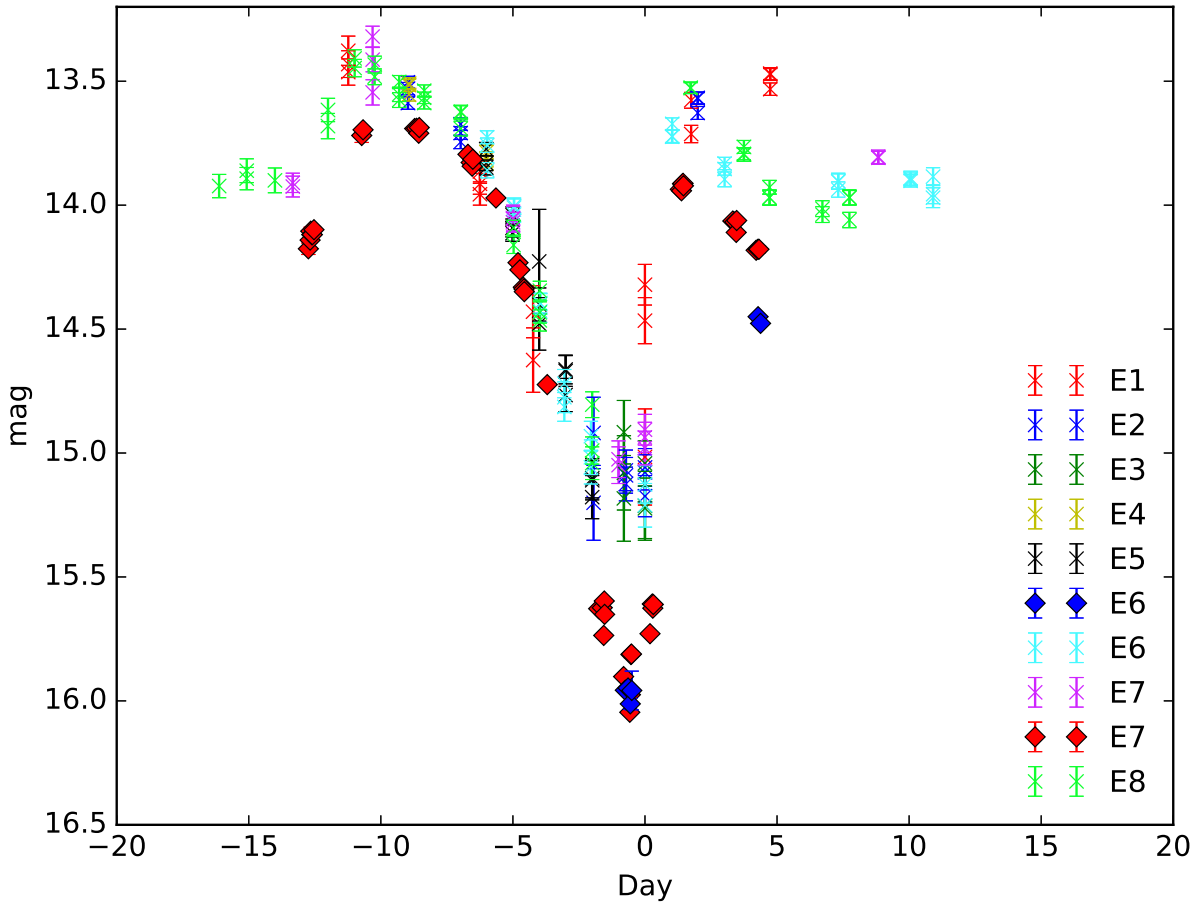

Figure 6. The dip events observed in the 2017-2018 season, where the diamonds and crosses represent the ZTF and ASAS-SN data, respectively. Two 2.5-mag dips, E6 and E7, were over plotted with other six similar dips, including E1, E2, E3, E4, E5 and E8. We aligned these events using their own fading slope, which have almost the same decreasing trends. With visual inspection, the minimum of the dips are chosen as the day of zero in the x-axis.

$\sim$ 2 mag, which could due to the issue of sampling of light curve around these events (i.e., the observations miss the epoches when the events reach to minimum). However, these dip events are aperiodically occurred in the range of $\sim$ 7 to $\sim$ 30 days. Using the entire light curves coverage from E1 to E8, the most likely event duration was found to be around 14.3 day estimated using the phase dispersion minimization (PDM, Stellingwerf 1978) method, as presented in Figure 7.

In the early epochs from 2011 to 2015, the dips B2 to B5 were individually recorded by Pan-STARRS or ASAS-SN, as seen in Table 4. A suspected dip B1 was also recorded in the DASCH light curve around 1934. Additionally, one more dip, A1, was caught by ZTF in 2018-2019 season. Before A1 occurred (2018 November 20), we have four successfully SEDM observations (see Figure 3). Unfortunately, there is a long queue of observing requests on SEDM until the end of our proposed observation run on 2018 November 27, so we did not have any further observation and missed the opportunity to catch the spectroscopic counterpart of this dip.

3.3. *Semi-Regular 0.5-Magnitude Outburst Events*

In addition the dip events mentioned in previous subsection, the long term light curves of HO Pup also exhibit a semi-regular $\sim$ 0.5 mag brightening events known as outbursts. These outburst events can been seen in Figure 2, for examples during the 2016 and 2017 seasons, and better visualized in upper panels of Figure 3 to 5. In Figure 8, we

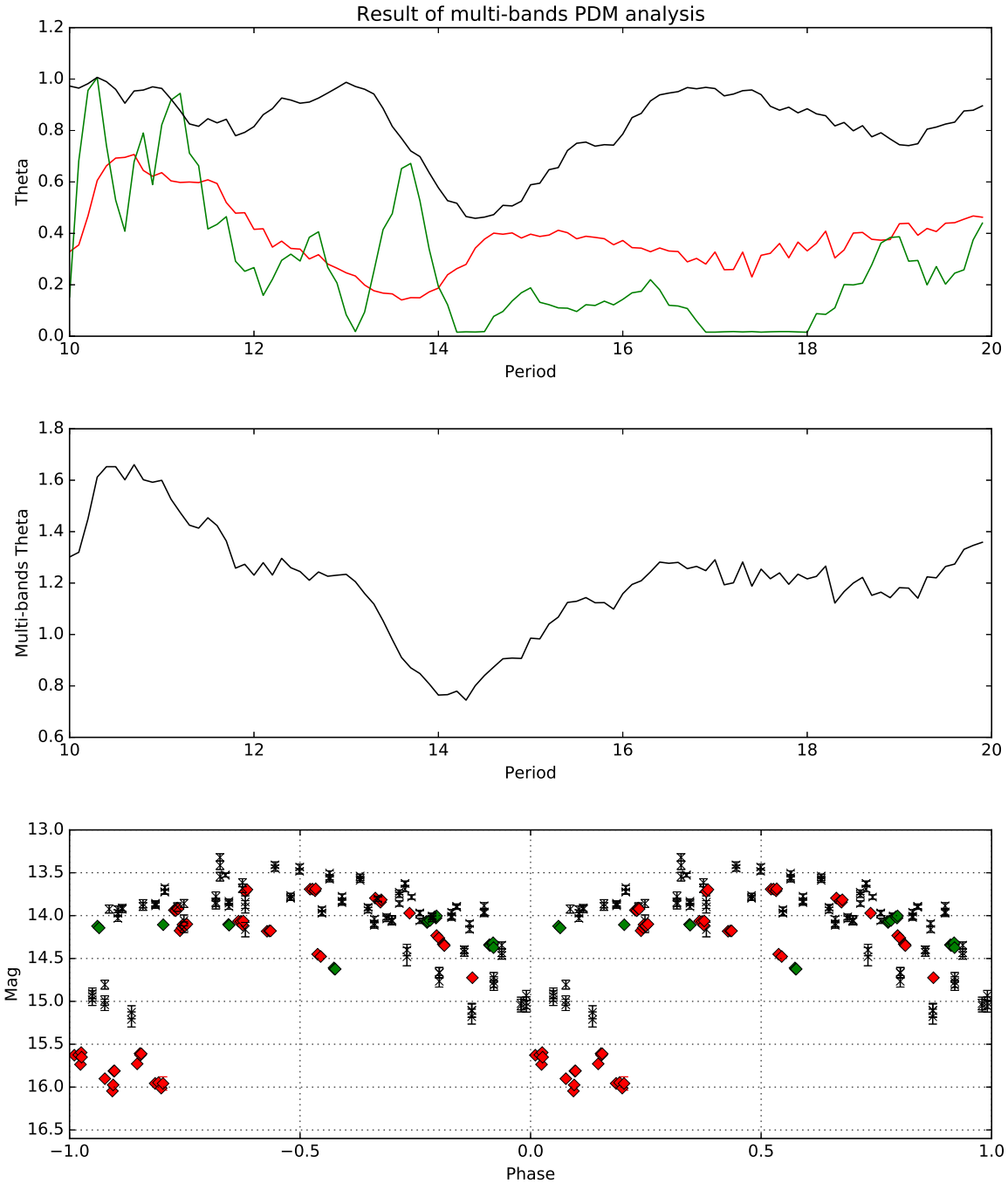

Figure 7. Multi-bands PDM analysis of the dip events. Upper panel: The periodogram of our PDM analysis as a function of trial periods (in days). The color curves include the observations from ZTF g-band (green color), ZTF r-band (red color) and ASAS-SN V-band (black color). Middle panel: Superposition of the periodograms for the three curves shown in upper panel, the minimum of this curve represents the best period. Bottom panel: The corresponding phased light curves using the best period found in the middle panel. The symbols are same as in Figure 2.

Table 4. Faintest measurements of each dip events.

JD	Date	Surveys	Mag	error	Band	Event No.
2427525.315	1934/03/28	DASCH	15.170	0.150	B	$B1$
2455645.785	2011/03/25	Pan-STARR	15.119	0.005	y	$B2$
2456016.802	2012/03/30	ASAS-SN	15.526	0.07	V	$B3$
2456596.153	2013/10/30	Pan-STARR	15.646	0.006	y	$B4$
2457038.010	2015/01/15	ASAS-SN	15.576	0.156	V	$B5$
2458007.137	2017/09/10	ASAS-SN	15.017	0.194	V	$E1$
2458021.849	2017/09/25	ASAS-SN	15.175	0.084	V	$E2$
2458033.880	2017/10/07	ASAS-SN	15.224	0.122	V	$E3$
2458049.806	2017/10/23	ASAS-SN	> 15.285		V	$E4$
2458049.435	2017/10/23	WISE	14.581	0.174	$W2$	$E4$
2458056.777	2017/10/30	ASAS-SN	15.178	0.087	V	$E5$
2458074.053	2017/11/16	ZTF	15.958	0.078	r	$E6$
2458074.771	2017/11/17	ASAS-SN	15.211	0.088	V	$E6$
2458101.029	2017/12/13	ZTF	15.975	0.01	r	$E7$
2458101.081	2017/12/13	ASAS-SN	15.05	0.074	V	$E7$
2458130.982	2018/01/12	ASAS-SN	15.041	0.066	V	$E8$
2458442.964	2018/11/20	ZTF	15.5	0.087	g	$A1$

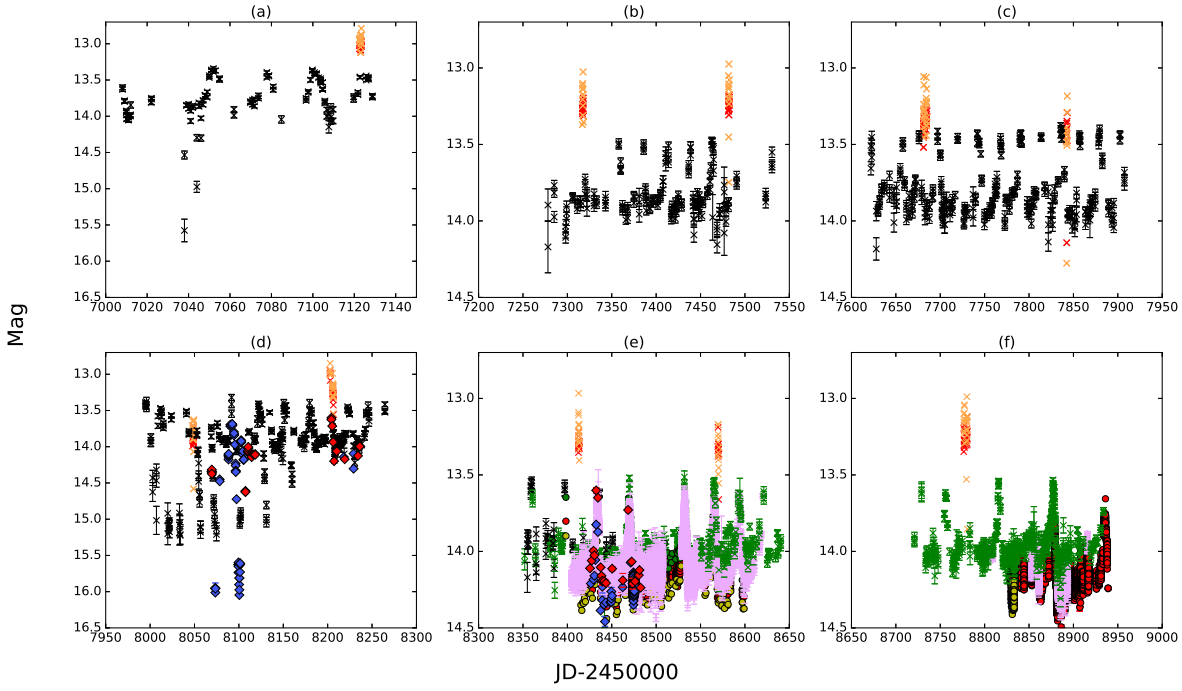

Figure 8. Same as Figure 2 but zoomed in for different seasons: (a) 2014-2015, (b) 2015-2016, (c) 2016-2017, (d) 2017-2018, (e) 2018-2019 and (f) 2019-2020.

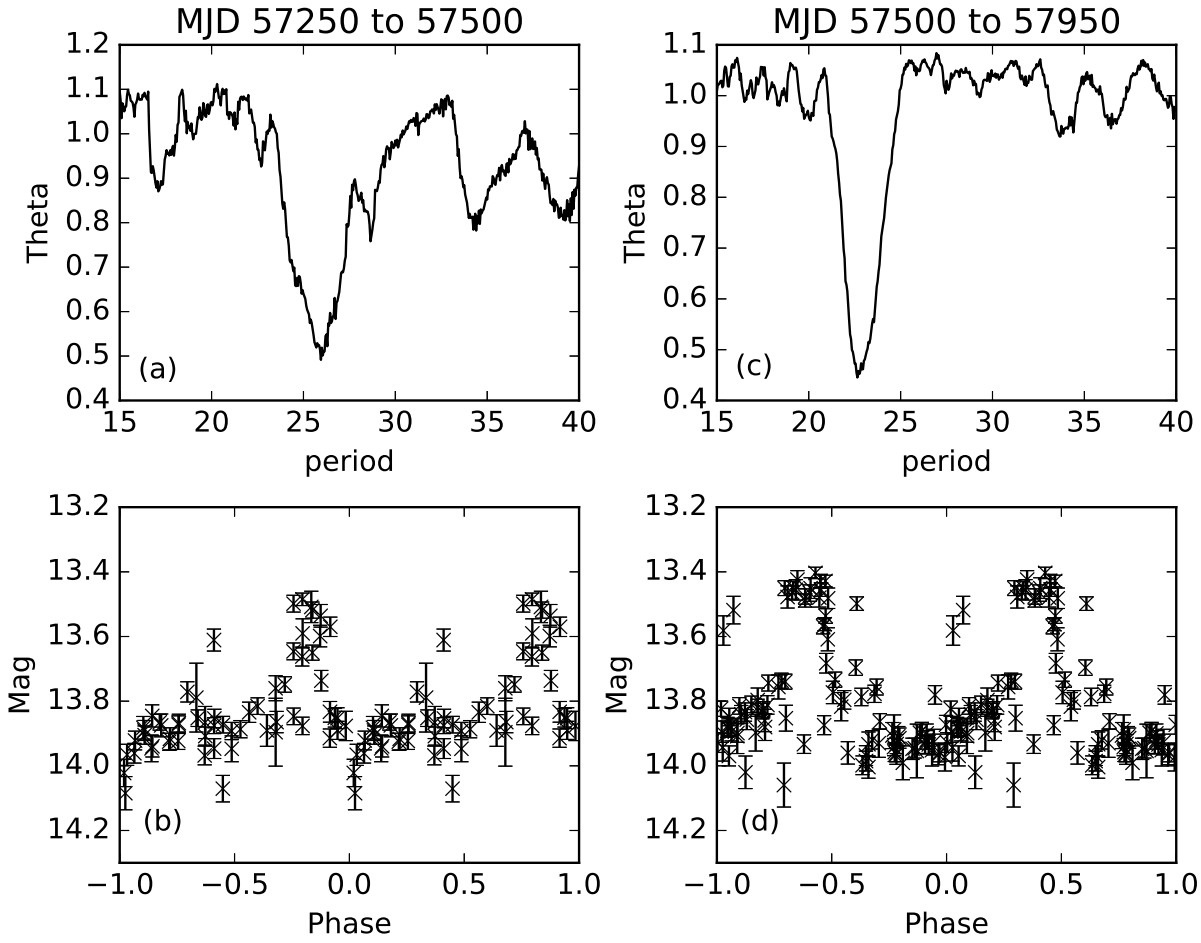

Figure 9. PDM analysis for the ASAS-SN light curves in 2015-2016 season (MJD: 57250-57500; left panels) and the 2016-2017 season (MJD: 57500-57950; right panels). The upper panels are the resulted PDM periodogram. The estimated best periods for these two seasons seem to change slightly from 25.9 days to 22.8 days. The bottom panels show the phased light curves based on these best periods.

split the ~ 7 years light curves of HO Pup into different segments. The ~ 0.5 mag outburst events are clearly showing in the light curves repeatedly with a duration between 21 to 61 days, as displayed in Figure 8 (a) to (f).

An initial analysis suggested these outburst events exhibit some periodicity but no single period can be determined. Therefore, we estimated the periodicity on different segments of the light curves using the PDM approach. These segments are similar to those presented in Figure 8. We derived a mean period of 25.9 days and 22.8 days for the light curves data in 2015-2016 (MJD: 57250 - 57500) and 2016-2017 (MJD: 57500 - 7950), respectively. The PDM analysis and the folded light curves for these two seasons are shown in Figure 9. For 2017-2018 (MJD: 57950 - 58300), the light curves are dominated by the dip events as presented in previous subsection, hence we excluded this part of the light curves for our PDM analysis. In 2018-2019 (MJD: 58300 - 58650), visual inspection suggested the periodicity of the brightening events varied sporadically with longest and shortest periods to be 37 and 26 days, respectively. Therefore we divided the light curves in 2018-2019 into three parts (in MJD): 58300 - 58485, 58485 - 58570 and those latter than 58570. The corresponding periods found by applying the multi-band PDM analysis are 35.6, 31.9 and 26.8 days, respectively, as presented in Figure 10. Finally, in the recent epoch 2019-2020 (MJD:58720-58933), the estimated period turns out to be 60.9 days as presented in right panels of Figure 10. It is worth to point out that these repeatable outburst events resemble the light curve of IW And-type stars (Kimura et al. 2020).

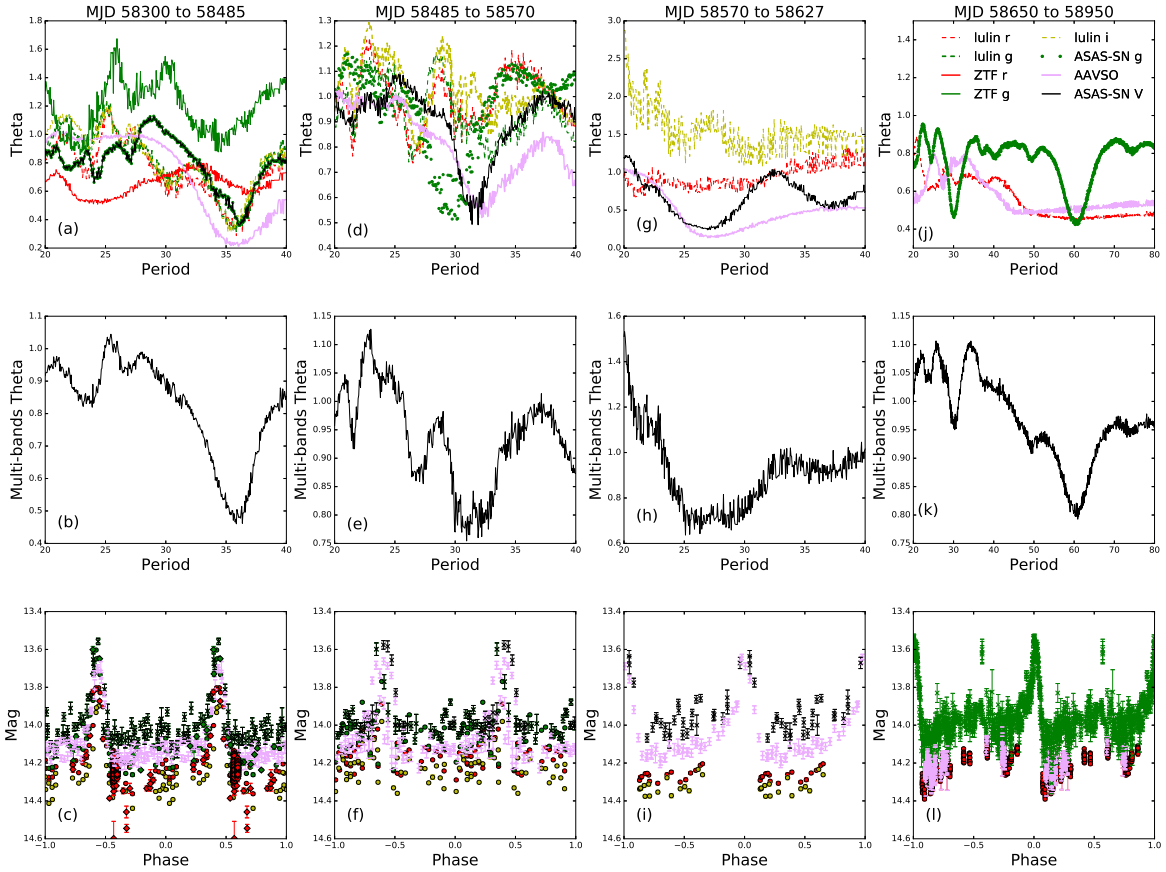

Figure 10. Multi-bands PDM analysis of outburst events in 2018 to 2020 seasons. Panels from left to right are for epoch (in MJD) from 58300 to 58485, from 58485 to 58570, from 58570 to 58627 and from 58650 to 58950, respectively. Upper panels show the PDM periodogram based on the individual multiband light curves. Middle panel shows the superposition of all photometric data. The rapid variation from 35.6, 31.9, 26.8 to 60.9 days are clearly seen in the middle panels. The bottom panels are the phased light curves with the same symbol as in Figure 2.

In case of spectroscopic observations, we have continuously taken spectrum every nights using CFHT/EsPADOnS before the optical light curve reached to its maximum brightness in one of the outburst events occurred in 2019 March (see Figure 4). We found that the strength, or equivalently the EW, of Hα line decreases while HO Pup became brighter, as shown in the spectra of the last two days in Figure 4.

3.4. *Color Variations*

We investigated the color variations of HO Pup using two sets of measurements. The relatively dense observations from ASAS-SN in g-band and AAVSO in V-band suggested that data points that were close in time can be used to estimate colors of HO Pup. Therefore, we selected data points from both surveys that were observed within 5 minutes to construct the $(g-V)$ colors. The second set of colors measurements was based on the data taken from the SLT telescope at the Lulin Observatory, where the gri-band images were always taken within 5 minutes. We constructed the $(g-r)$, $(r-i)$ and $(g-i)$ colors based on this set of observations. All of these colors measurements are presented in Figure 11, which suggested there are some variability presented in the colors of HO Pup. Interestingly, it seems that there is no difference in the colors of HO Pup when it underwent the ~ 0.5 mag outburst events (see subsection 3.3, as shown as blue points in panel (b) of Figure 11) or HO Pup is at its "normal" brightness (the standstill phase; red points in panel (b) of Figure 11).

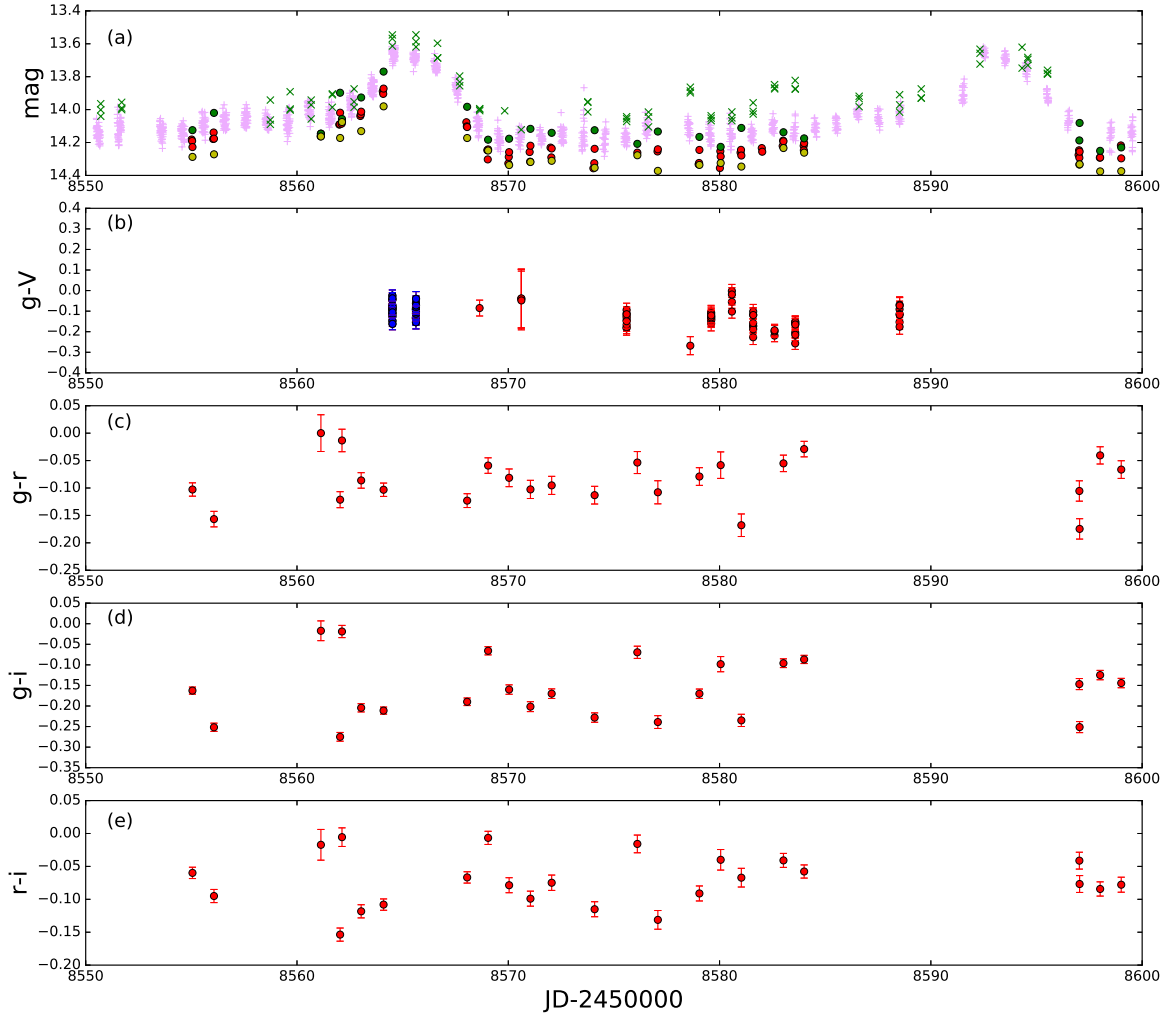

Figure 11. Panel (a): A segment of the light curves for data taken in 2018-2019 season, the symbols are same as in Figure 2. Panel (b): The $(g-V)$ color curves based on the nearest ASAS-SN and AAVSO observations. The blue points represent the colors at the ~ 0.5 mag outburst events discussed in sub-section 3.3, while the red points are those outside such events. Panel (c) to (e): the $(g-r)$, $(g-i)$ and $(r-i)$ colors based on the near simultaneous SLT observations taken at the Lulin Observatory.

To further quantify the colors variation with brightness, we plotted the magnitudes as a function of colors (i.e. the color-magnitude diagram, CMD) in Figure 12. In all these optical colors, again the blue data point were those corresponding the ~ 0.5 mag outburst events and the red data points were taken at the standstill phase. As can be seen from panel (a) of Figure 12, the colors at these two phases cover a very similar range. Furthermore, all of the colors present a trend such that colors become bluer when HO Pup becomes brighter, especially for the $(g-i)$ colors shown in panel (c) of Figure 12.

3.5. *Variabilities at Short Time Scale*

In addition to the dip events and outburst events, as presented in sub-section 3.2 and 3.3 respectively, short term variabilities were also found in the light curves of HO Pup during its standstill phase. For example in late December of 2018, ZTF performed intense observations on the Galactic Plane which included HO Pup. Therefore, intense light

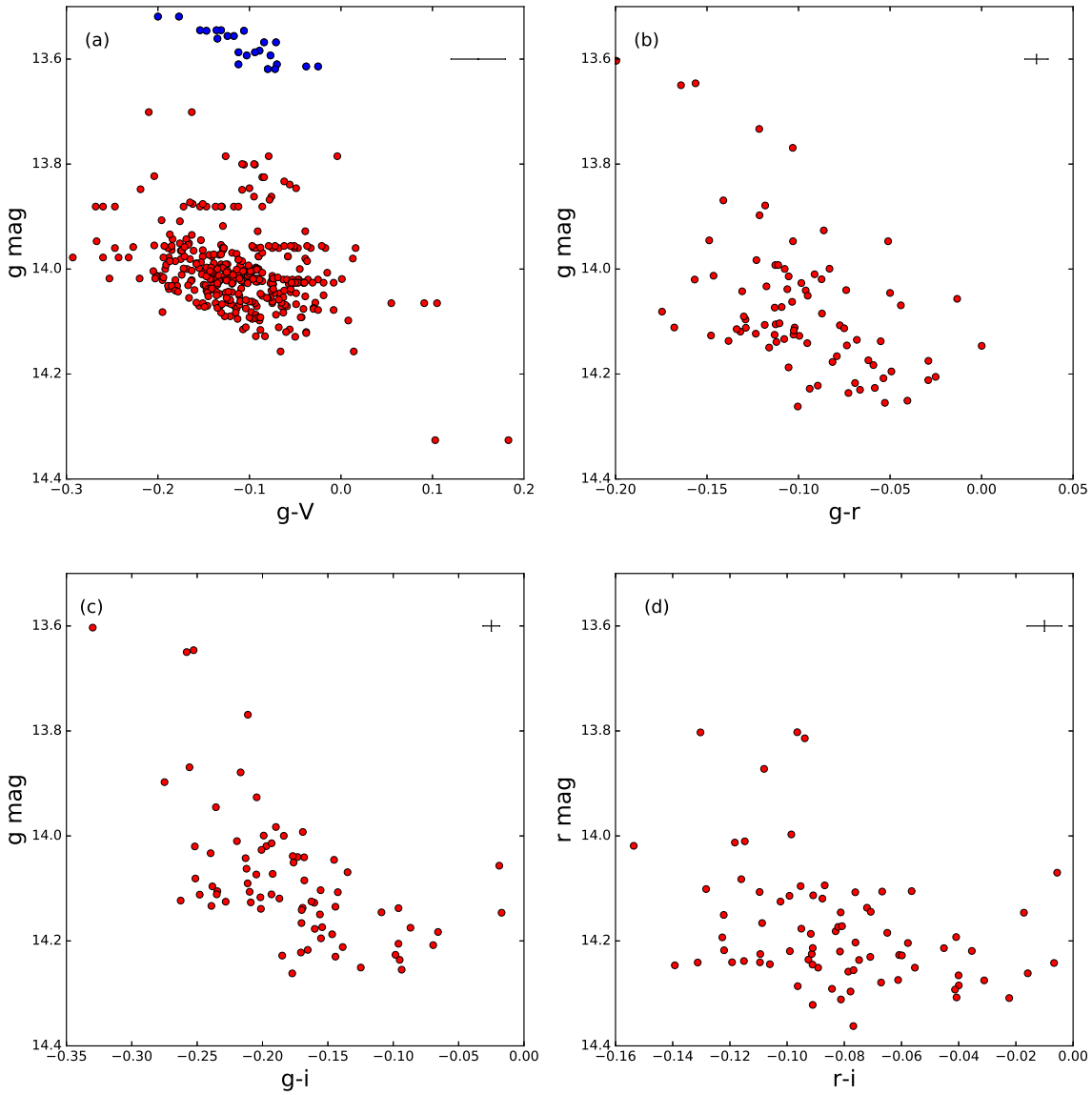

Figure 12. The color magnitude diagrams (CMD) of HO Pup. The representative error bars of colors and magnitudes are shown in the upper right corners of these four CMDs. The g- and V-band data in panel (a) were taken from ASAS-SN and AAVSO, respectively. The intense observations from both surveys allow us to separate the data points for those occurred at the $\sim$ 0.5 mag outburst events (blue points) as discussed in sub-section 3.3, and those outside these events (red points). In panel (b) to (d), the gri-band data are based on the SLT observations taken at the Lulin Observatory. All of these CMDs show that HO Pup becomes bluer when it gets brighter.

curves data were available from ZTF on 2018 December 22 and 23, with 280 and 136 measurements taken within 2 hours in the r-band, respectively (see Figure 13). An hour-scale sinusoidal variability with $\sim$ 0.1 mag to $\sim$ 0.2 mag amplitude was revealed in this set of ZTF light curve. Similar variability can also be seen from the AAVSO light curve, even though the cadence of AAVSO data is not as high as ZTF in these two nights. On December 22, we have

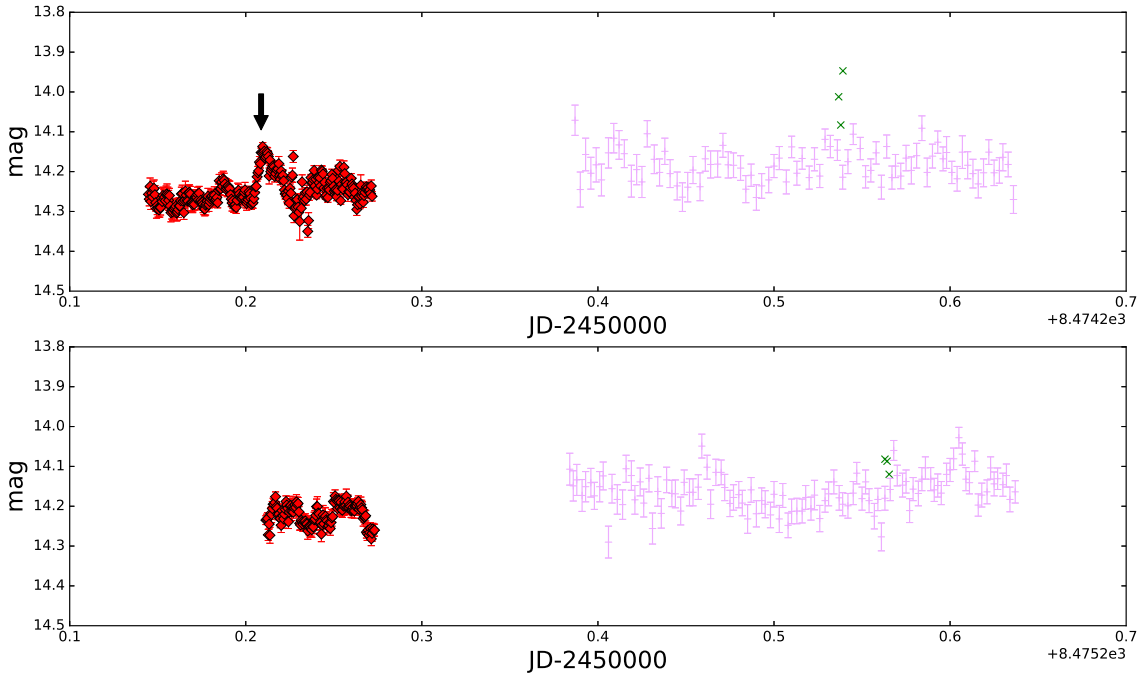

Figure 13. Same as Figure 2 but with the time scale zoomed into two days. Based on the ZTF data taken in 2018 December, some variabilities in the timescale of hours are clearly observed. In December 22 (upper panel), we see a flipped S-shaped event (indicates by an arrow) lasting about an hour. In the next day, December 23 (lower panel), the ZTF light curve obtained in two hours shows a variability with sinusoidal-like profile. Even with lower cadence or photometric precision, similar variations are also seen in the AAVSO light curve.

also observed an event with sudden increase of amplitude with a flipped S-shape profile. Due to ~ 2 hours time span of the ZTF light curves on these variability, we do not perform periodicity analysis for these two nights.

To verify the short timescale variability of HO Pup light curve, we performed intensive monitoring of HO Pup with the SLT telescope in late 2019 to 2020. Such intensive observations were done in single r-band filter with 30 seconds exposure time, continuously for 2 to 5 hours in every clear nights. Using both PDM and Lomb-Scargle periodigram algorithms, the most obvious resolved periodicity are 3.9 days and 50 minutes respectively, as seen in Figure 14 and 15. Data taken around the outburst (for 5 nights) and about an hour before the dawn were removed in order to maintain high quality light curve to detect the short timescale variability. In addition to the 3.9 days and 50 minutes variabilities, two very weak periods, at 20 minutes and 90 minutes respectively, were also detected but cannot be confirmed.

3.6. *Polarization Variation*

We have also observed variations on polarization for HO Pup. Based on polarization level P and position angle θ measured from Lulin Observatory (see Table 3), a small and yet significant polarization was observed on 2018 October 24 and 26. However, the polarization drops back to an insignificant value on 2018 October 25 and 2018 October 28. The observed variation in polarization suggested Ho Pup exhibits intrinsic polarization.

4. DISCUSSION

4.1. *Spectral and Luminous Class Identification*

Prior to our work, classification of HO Pup in the literature was done via inspection of it light curves, as either a Be star with GCAS-type variability (Samus et al. 2017) or as an IW And-type DN (Kimura et al. 2020). Here, we first estimated its spectral and luminous class using spectral energy distribution (SED) fitting together with distance estimation based on the Gaia Data Release 2 (DR2) parallax measurement (1.6165 ± 0.0311 mas, or $d = 618.6$ pc,

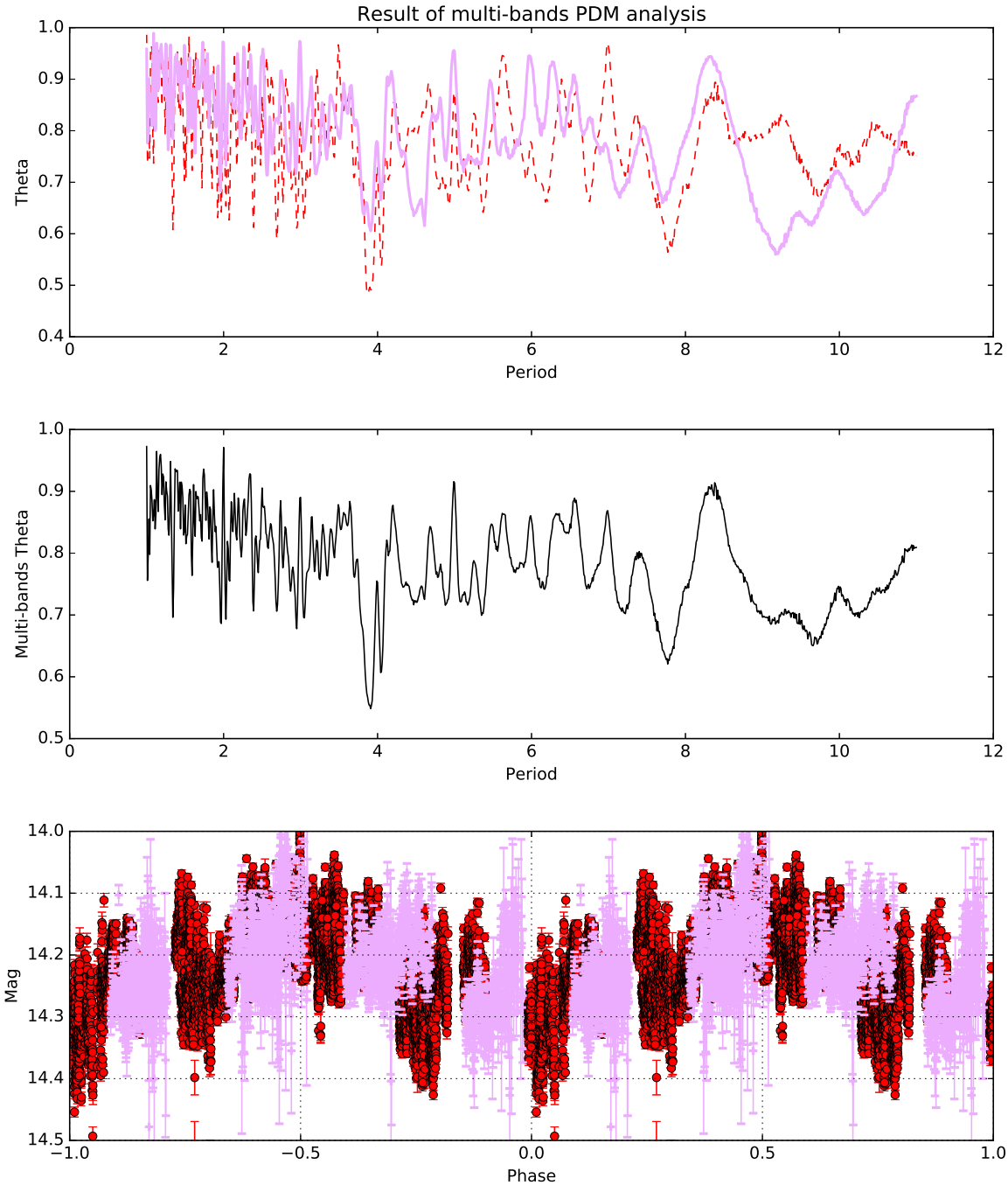

Figure 14. Multi-bands PDM analysis of the oscillatory variation at the timescale of days. The line styles shown in the upper panel are same as in Figure 10 (j). A 3.9 days period is clearly detected from light curves based on two individual observations (upper panel), as well as the superposition of both observations (middle panel). The bottom panel is the phased light curves folded with the detected 3.9 days period, at which the symbols are same as in Figure 2, revealing a sinusoidal shape light curve.

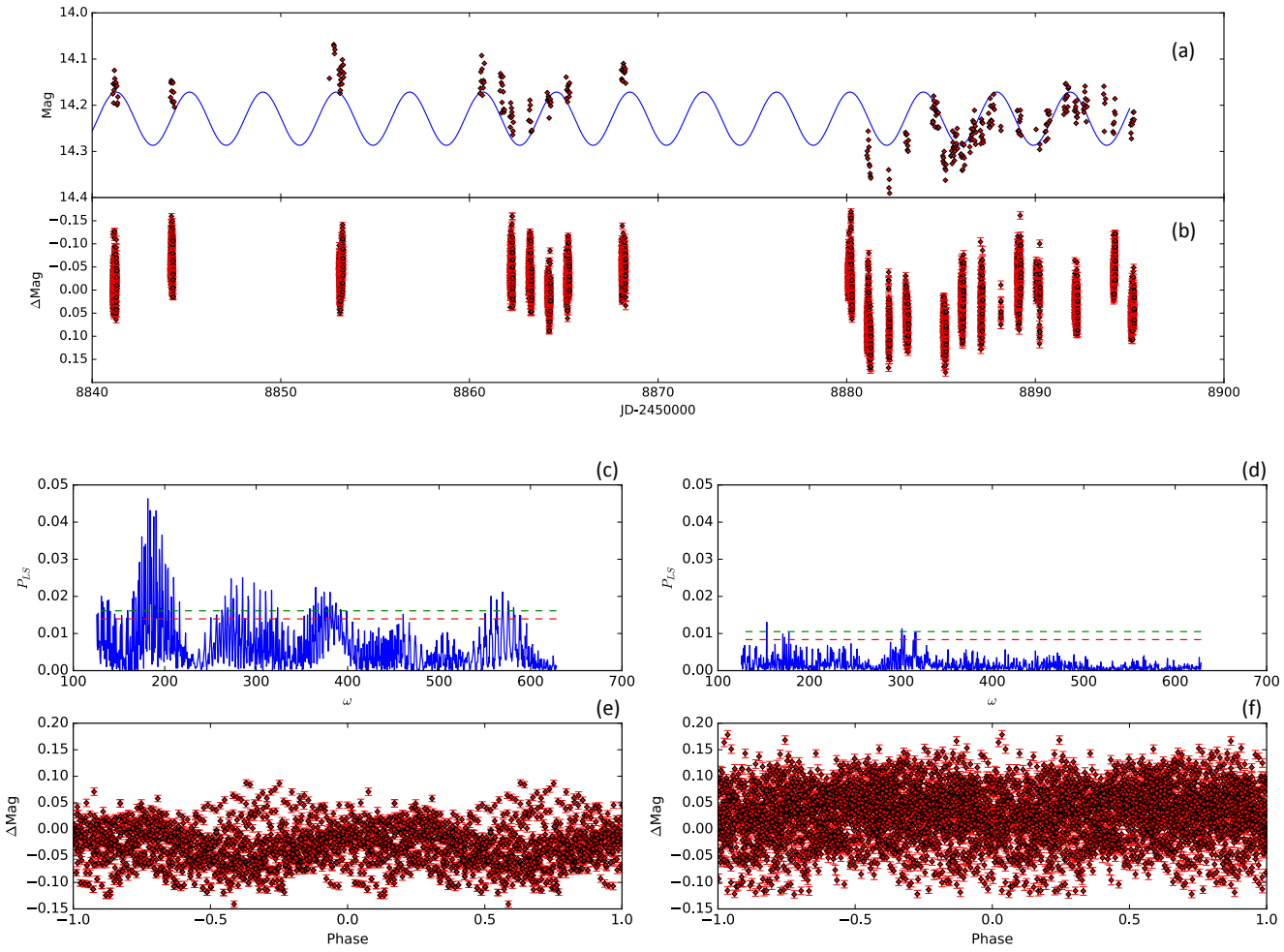

Figure 15. The variability of HO Pup down to timescale of hours. Panel (a) presents the SLT r-band photometric data (red dots) taken from 2019 December to 2020 March. The blue curve represents the 3.9 day cycle fitted with a sinusoidal function. (see Figure 14). To uncover the variability shorter than one day, this light curve has been subtracted with the sinusoidal function of 3.9 days, shown in panel (b). After removing the 3.9 days cyclic variations, we found a new cycle of 50 minutes variations using Lomb-Scargle periodogram analysis, based on the light curve data taken from 2019 December to 2020 January, as shown in panel (c). As can be seen from this panel, the variation signal is well above the false alarm probability (FAP, indicated by the red and cyan dashed lines for the 95% and 99% FAP, respectively). The variability with 50 minutes periods can be easily seen in the phased light curve as presented in panel (e). However, such 50 minutes variations were barely resolved or undetected for the data collected between 2020 February and March, as evident in panel (d) and (f). Instead, complicated variations can be seen in the nightly chunks of light curves data within this period of observations.

Gaia Collaboration et al. 2018). The observed SED of HO Pup was constructed using available broadband photometry covering from near-UV to mid-infrared. In Table 5 we listed all available broadband photometric data of HO Pup queried within 1″ radius using the `VizieR` photometry viewer (Ochsenbein et al. 2000). As shown in the Figure 16, the SED peaked between near-UV and B band indicates it is a hot early-type star.

Assuming HO Pup is a luminous B-type main sequence star, fitting these broadband photometric data with a theoretical SED model (Kurucz 1993) suggested the spectral class of HO Pup have to be B1V (Figure 16), with the corresponding extinction of $A_V = 0.5$ and at a distance of 16 kpc. However, this distance is inconsistent with the Gaia DR2 distance.

If the Gaia DR2 distance is correct, we then derived a $M_V \sim 5.1$ mag for HO Pup by adopting an apparent magnitude of $m_V = 14$ mag and an extinction of $A_V = 0.1$ mag (Green et al. 2019). This value of M_V is consistent with the luminosity of some faint blue stars (e.g., hot subdwarf stars; see Geier et al. 2019). As can be seen in Figure 16, the

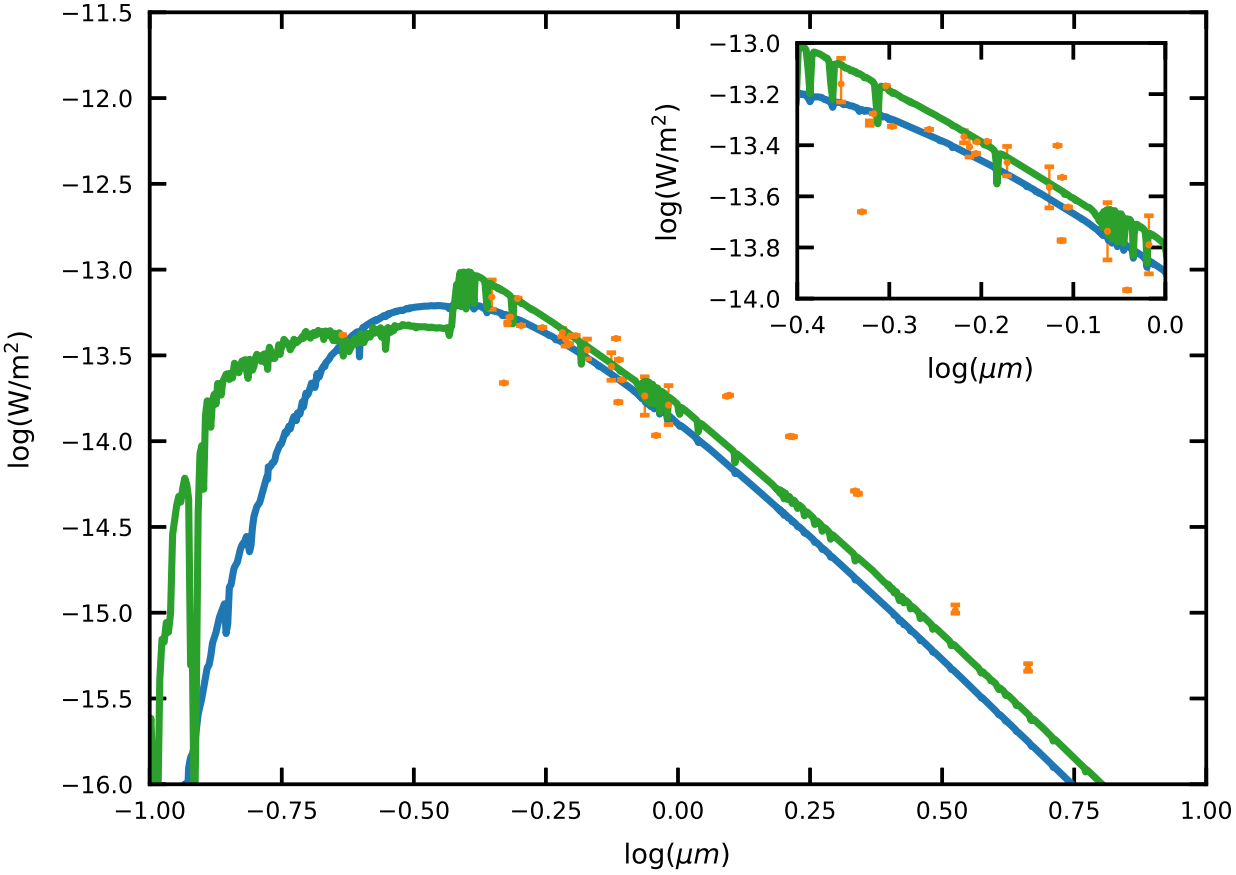

Figure 16. The observed SED of HO Pup (orange points from broadband photometry) is fitted with Kurucz (1993) stellar models with two luminosity classes, presuming of an object consisting of a B1V dwarf (blue) or a sdB (green) with effect temperature of 14,000 K, assuming a distance of 16 kpc with $A_V = 0.5$ and 618 pc with $A_V = 0.1$, respectively. The photometric data are listed in Table 5. The inset figure shows the zoomed in portion in the optical band.

SED data of HO Pup can also be well fitted with a faint blue object with 14,000 K at a distance distance provided by Gaia DR2. Therefore, the possibility of HO Pup being a Be star is ruled out.

As presented in previous sections, the IW And-type phenomenon can be seen in the light curves of HO Pup collected in our work (as well as in Kimura et al. 2020). HO Pup is not the only case known to have sub-luminous companion among the IW And-type stars. In fact, the prototype object, IW And, is also a binary system likely with a subdwarf B (sdB) star as a companion (Meinunger 1980).

4.2. *Spectroscopic Characteristics*

Spectral features of the hot sub-luminous stars are also seen in HO Pup. Broad Balmer absorption lines are commonly shown on the spectra of hot subdwarf (Geier et al. 2013; Mason & Howell 2016), since they are core-helium-burning objects ($\sim$0.5 $M_\odot$) surrounded by a thin hydrogen shell ($\leq$ 4% by mass). As seen in Figure 5, this characteristic is obviously shown in our spectra up to Hζ. Other helium and metal lines including He I, He II, Fe I and Mg I appear in our spectra as well. As a core exposed object, helium lines and other metal lines are expected to be present in the spectra of HO Pup, similar to the object studied in Schindewolf et al. (2018, a sdO star with enrichment in heavy metal.).

Table 5. Adopted broadband photometric data for HO Pup to be used in SED fitting.

Band	$\lambda(\mu m)$	mag	error	reference
NUV	0.231	15.135	0.011	Morrissey et al. (2007)
Bj	0.435	15.16	0.42	Lasker et al. (2008)
B	0.444	14.233	0.57	Zacharias et al. (2012)
B	0.444	13.8	0.43	Lasker et al. (2008)
B	0.444	13.240	···	Zacharias et al. (2005)
Bf	0.468	13.86	0.44	Lasker et al. (2008)
g	0.481	14.079	0.556	Geier et al. (2019)
g	0.481	14.237	0.192	Heinze et al. (2018)
g	0.481	13.818	0.273	Wolf et al. (2018)
g	0.481	14.199	0.204	Chambers et al. (2016)
G_{BP}	0.532	14.121	0.029	Gaia Collaboration et al. (2018)
V	0.551	14.082	0.49	Zacharias et al. (2012)
V	0.551	13.340	···	Zacharias et al. (2005)
r	0.617	14.085	0.013	Heinze et al. (2018)
r	0.617	13.974	0.272	Wolf et al. (2018)
r	0.617	14.043	0.008	Chambers et al. (2016)
r	0.617	14.074	0.42	Zacharias et al. (2012)
R	0.658	14.170	···	Zacharias et al. (2005)
G	0.673	14.083	0.009	Gaia Collaboration et al. (2018)
i	0.752	14.391	0.003	Wolf et al. (2018)
i	0.752	14.150	···	Heinze et al. (2018)
i	0.752	14.118	···	Chambers et al. (2016)
i	0.752	13.887	0.10	Zacharias et al. (2012)
In	0.784	14.04	0.43	Lasker et al. (2008)
G_{RP}	0.797	13.833	0.049	Gaia Collaboration et al. (2018)
z	0.866	14.586	0.003	Wolf et al. (2018)
z	0.866	14.363	0.015	Heinze et al. (2018)
z	0.866	14.311	0.017	Chambers et al. (2016)
y	0.962	14.354	0.054	Heinze et al. (2018)
y	0.962	14.327	0.050	Chambers et al. (2016)
J	1.25	13.300	0.026	Skrutskie et al. (2006)
H	1.65	13.137	0.027	Skrutskie et al. (2006)
K_s	2.15	13.152	0.037	Skrutskie et al. (2006)
W1	3.40	13.480	0.028	Cutri et al. (2012)
W2	4.60	13.358	0.038	Cutri et al. (2012)
W3	12.00	12.564	0.471	Cutri et al. (2012)

Moreover, we found CV signatures from the spectra of HO Pup, such as our P200/DBSP spectrum, taken at the outburst right after the maximum brightness, with weak emission cores presented in most of the broad Balmer absorption lines. Szkody et al. (2013) observed two CVs, IW And & V513 Cas, in their outburst phase, at which their Balmer lines were nearly the same as in HO Pup. Beyond the hydrogen features, there is a double-peaked, bumpy and shoulder-like feature in between Hβ and Hγ, which include the lines of C III, N III (known as Bowen fluoresces at 4640 Å) and He II (4731 Å). This is an unique blended emission line that can be revealed especially during the phase of CV outburst. In the phase of standstill, the Bowen features become much insignificant as seen in the BOAO/BOES spectrum, along with shallower Balmer absorption. Hessman et al. (1984) reported the time-resolved spectroscopic observations from outburst to standstill for a classical CV SS Cyg, showing the strength of the emissions from Bowen fluoresces declining to the continuum level. The similarity of HO Pup spectra features and these CV strongly suggested HO Pup is a CV with a hot sub-luminous companion. Additional two spectroscopic differences between outbursts and

standstill are not seen in the literature including a weaker H I 6678 Å line shown in the standstill phase and the Na I doublet showing up during the outbursts (See Figure 5).

4.3. *Outbursts Followed by Dips*

One of the main light curve features among IW And-type stars is some of the outbursts would be followed by a single deep dip event. However, Kimura et al. (2020) excluded this situation in their tilted disk model, due to the difficulty of reproducing such one time dip event in the model. On the other hands, to explain the similar phenomenon as seen in the light curve of V513 Cas, a mass transfer rate depended model has been proposed by Hameury & Lasota (2014) to reproduce the observed light curves of small brightening followed by a deep dip event. We suggest that the same mechanism could be responsible for the observed light curves of either V513 Cas or HO Pup, or both.

The shapes of the dip events are almost the same for HO Pup and V513 Cas, but the former has a large cycle variation. The cycles of outburst events range from 7 to 31 days for HO Pup. On the other hands, all cycles of V513 Cas last about 100 days. We believe the mass transfer rate dominated by the secondary donor star surely plays a major role here. To better understand the physics mechanics underlying the instability of the accretion process (such as the surface activity of the secondary star), additional long term spectroscopic monitoring should be carried out on these stars.

4.4. *Outbursts Followed by Standstill*

Except the dip events occurred in the 2017-2018 season, and a few dips in other epochs, HO Pup have very similar behavior like a normal DN with a semi-regular outburst frequency. For those light curve segments without dip events, the duration of the outbursts varying between 23 to 61 days. Using the model presented in Kimura et al. (2020), this style of variation can be explained if we consider HO Pup as an IW And-type star. In brief, the accretion disk of this kind of object is tilted to the orbital plan, so accretion flow can reach to entire disk including the inner part and the outer part of the disk. With an increasing accumulated mass, the inner disk is almost always in hot state, so most of time HO Pup is in standstill phase with optical brightness around 14 mag. On the other and, the outer part of accretion disk is in cool state before enough mass accreted to light it up. As can be seen in Figure 12, the colors of HO Pup become bluer as the star getting brighter. We suggest that both of the brightness variation and the temperature of the disk are dominated by the mass transfer rate. We see a hotter HO Pup when it becomes brighter either in outburst phase or in standstill phase. Bowen fluoresce and other metal lines that can be seen in the outburst phase may indicate the hot state of both inner and outer part of the accretion disk.

The hot disk effect is also shown up in mid-IR from WISE observations. The outbursts in mid-IR is almost varying together with the optical ASAS-SN V band light curve (see Figure 17), since the entire continuum rise up together with disk temperature. Therefore, the emission metal lines, including Bowen fluorescence, become stronger in the spectrum when taken during the outburst phase.

The tilted accretion disks model with cycle-limit oscillation proposed by Kimura et al. (2020) can explain both of the outburst events and the 3.9 days cycle seen in the light curve of HO Pup. In the tilted disk model, the accretion flow will not only fall into the inner disk but also to the outer disk. However, unstable accretion rate can make IW And-type stars different from DN or nova-like objects. With enough mass supply, the inner part of disk can stay in hot state in both standstill and outburst phases. Once the mass threshold was achieved in the outer disk, outburst could occur from inside to outside of the disk, or known as inside-out outburst (Kimura et al. 2020). The 0.5-mag brightening was then shown up in the light curve. Due to the instability of the accretion rate, the entire disk can be cooled since little mass left in the disk, and hence the brightness can drop dramatically. Even the outburst cycle is about 20 to 60 days with predictable pattern on the duration from current outburst to the next, we yet have a good scenario to explain the cycle variability if we considering the tilted disk model presented in Kimura et al. (2020).

Unlike other known IW And-type stars, HO Pup has no small dips showing in the standstill phase. A smooth oscillation can be visually seen from the phased light curve (see lower panels of Figure 10). This oscillation is the 3.9 days cycle that we detected from the PDM analysis (see Figure 14). Interestingly, the phenomenon can be accounted for using the tilted disk models as well (the model C with the highest inclination as presented in Kimura et al. 2020). Since the accretion disk is highly tilted, then the inner disk could receive a much higher mass supply than the disk that is less tilted.

Among the outburst events seen in HO Pup, most of the outbursts were followed by a standstill phase. However, almost all outbursts in 2017-2018 season were followed by a dip event. If we consider HO Pup as a IW And-type star

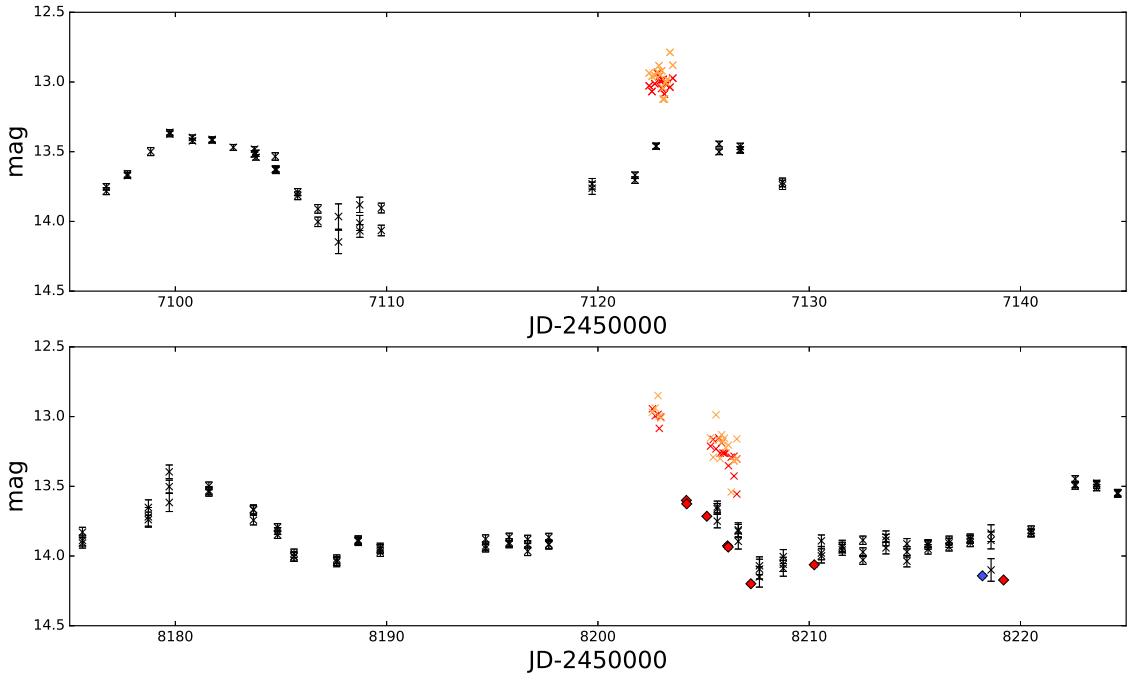

Figure 17. Same as Figure 2 but zoomed in for the two ~ 0.5 mag outburst events as observed with the WISE data in 2015 (upper panel) and 2018 (lower panel).

with a tilted accretion disk, we have witnessed a long sequence of inside-out outbursts with eight complete samples of dip events (see Table 4). Since E2, the intervals between two dip events, or the duration, were getting longer from 12 days to 30 days, deviating further from the approximated duration of 14 day as estimated from PDM analysis (see Figure 7).

Based on the polarimetric observations taken during the standstills phase (see Figure 3), HO Pup shows intrinsic optical polarization variability, at which the polarized light include the star's light and the light from the disk. Presence of magnetic field or disk scattering may account for the polarization. Despite the variation of polarization level, the polarization percentage P at four different nights are all measured to be $< 1\%$ in our r and i band TRIPOL2 data. Szkody et al. (1982) show the same extend of polarization level among 3 DNs in their standstill phase.

4.5. *Similarity to Be stars*

Previously, HO Pup was considered as a Be star based on its GCAS-like light curves. However, those incomplete light curves were sparsely sampled in the past, as shown in Figure 2, that could be responsible for the mis-classification of HO Pup as a Be star. HO Pup has a better observation coverage since 2016, therefore its DN nature can be revealed by Kimura et al. (2020) from the dense sampling of the light curve.

Since both of the Be stars and IW And-type stars are hot early type stars with hydrogen and helium lines, as well as exhibit irregular and abrupt photometric variations (e.g., due to presence of disk), these two type of stars share a number of common observational features. As evident from the case of HO Pup, an IW And-type star could be mis-classified as a Be stars based on a limited observational evidence (and/or vice versa). In Table 6, we compared and summarized some of the important observational features of Be stars, IW And-type stars and HO Pup. For example, Be stars could display regular dip events due to eclipsing as in the case of RW Tau with dips fainted by ~ 4 mag (Bookmyer 1977). On the other hands, the deepest dip event observed on IW And-type stars is fainted by ~ 3 mag (Kato 2019) without cyclic variations. The observed dips events of HO Pup, without regularity of the cycle of the dip events (from 12 to 30 days), resembled higher similarity to IW And-type stars rather than the eclipsing Be stars. Furthermore, for the outburst events that were not followed by dip events, IW And-type stars have a much

Table 6. The spectroscopic and photometric features shown in Be stars, IW And-type stars and HO Pup

	Be Stars	IW And Stars	HO Pup
Number	∼3000	6	1
Hydrogen lines	yes	yes	yes
Helium lines	yes	yes	yes
Spectral type	early	early	early
Bowen fluorescence	no	yes	yes
Dip δM_v	4 mag (RW Tau)	3 mag	2.5 mag
Dip cycle		15-55 days (ST Cha)	7-30 days
Outburst δM_v	< 0.5 mag	0.5-1 mag	0.5 mag
Outburst cycle	71 days (δ Sco)	15-200 days	23-61 days
Outburst duration	2-1000 days	a few days	∼5 days

more regularity in their outburst phase (with outburst cycles range from 15 to 200 days) when compare to Be stars displaying GCAS-type light curve at which the outbursts are more secular.

Although the outburst duration of IW And-type stars are mostly much shorter than Be stars, they have similar inverse correlation between photometric brightness and spectroscopic line emission. For IW And-type stars, the brightness variation is dominated by accretion disk along with the growth of disk atmosphere, so we see the growth of the hydrogen absorption. On the other hand, for Be stars, disk extinction dominates the brightness variation (Sigut, & Patel 2013). When the disk dissipates out, we see brighter Be stars with less amount of line emitting material surrounded. The inside-out mass processing is what a Be star forming a "decretion" disk surrounding the host star (Rivinius et al. 2013). It is very interesting to see the two very different kind of disk (accretion disk and decretion disk) showing similarly photometric and spectroscopic behavior.

We see a similar interplay in the eight nights of our CFHT/ESPaNDOnS observations. During these observations, HO Pup experienced a transition from 14 to 13.5 mag at the same time the EW of Hα line strength decreased from $-6.4\AA$ to $-1.2\AA$ (see Figure 4). A similar behavior between Hα emission line strength and photometric brightness was also clearly observed in another Be star, V438 Aur (Labadie-Bartz et al. 2017). However, the obscured phase of HO Pup is up to ~ 36 days which is far less than V438 Aur (more than 2000 days).

Therefore, as summarized in Table 6, we cannot easily distinguish IW And-type stars from the field (luminous) Be stars without knowing the distance, because they share the same color, and nearly the same spectral features. With the low sampling of light curves and limited spectroscopic observations, neither photometric nor spectroscopic data can be used to distinguish possible IW And-type stars from a list of faint Be stars. If we observe any other unknown IW And-type stars, or more general DN with sub-luminous OB companion, with low sampling light curve (as in the case of HO Pup before 2010), there is a large probability that these stars would be classified as Be stars based on their GCAS-like light curve. Spectroscopic observations might also be difficult to separate these two classes of stars, unless the spectra were taken during the outburst phase which contain unique features of metal lines (like Bowen fluorescence) for CV. Since the outburst phases of a CV last only a few days, as compared to Be stars that can last for longer than 10 days, there is a narrow observing window for taking the spectra for these objects.

5. SUMMARY

Instead of considering as a Be candidate, we confirmed that HO Pup is an IW And-type DN accompanied with a sub-luminous star based on the light curve pattern, spectroscopic characterizations along with the Gaia DR2 distance and SED fitting. To resolve the variability nature superposed with multiple timescale, we have collected nearly 28,700 data points for HO Pup crossing about a century. Outbursts followed by standstill phase or followed by dip events are very likely reflecting the variation of mass transfer rate from the donor star. However, mechanisms that causing the changing of mass transfer is still unknown. To shed light on the stellar physics behind light curve of IW And-type stars, further well-covered spectroscopic monitoring along with intense photometric observations are highly desirable.

This work is partly supported by the Ministry of Science and Technology (Taiwan) under grants of 107-2119-M-008-014-MY2, 107-2119-M-008-012, and 108-2811-M-008-546. We thank Abert Kong for pointing out the DASCH light curve. We also thank the discussions with Yi Chou, Wen-Ping Chen, Shih-Yun Tang, Michihiro Takami, Chi-Hung Yan, Paula Szkody and Melissa Graham on this work, as well as suggestions from an anonymous referee to improve the manuscript.

Based on observations obtained with the Samuel Oschin Telescope 48-inch and the 60-inch Telescope at the Palomar Observatory as part of the Zwicky Transient Facility project. ZTF is supported by the National Science Foundation under Grant No. AST-1440341 and a collaboration including Caltech, IPAC, the Weizmann Institute for Science, the Oskar Klein Center at Stockholm University, the University of Maryland, the University of Washington, Deutsches Elektronen-Synchrotron and Humboldt University, Los Alamos National Laboratories, the TANGO Consortium of Taiwan, the University of Wisconsin at Milwaukee, and Lawrence Berkeley National Laboratories. Operations are conducted by COO, IPAC, and UW. SED Machine is based upon work supported by the National Science Foundation under Grant No. 1106171

This research relied on the SIMBAD and VizieR catalogue access tool and the Aladin plot tool at CDS, Strasbourg (France), and NASA ADS bibliographic services. This publication makes use of data products from the Wide-field Infrared Survey Explorer, which is a joint project of the University of California, Los Angeles, and the Jet Propulsion Laboratory/California Institute of Technology, funded by the National Aeronautics and Space Administration. We also made use of data collected at Lulin Observatory, partly supported by MoST grant 108-2112-M-008-001. We sincerely thank the staff and queue observers (Chi-Sheng Lin, Hsiang-Yao Hsaio and Wei-Jie Hou) at the Lulin Observatory for carried out the observations with the SLT telescope. We thank the observer at the P200 Telescope, Marianne Heida, for taking the P200/DBSP spectrum. We also appreciate the achieve and online catalogs provided by ASAS-SN, AAVSO and Pan-STARRS, making this investigation possible for in much longer baseline and/or better time coverage. The DASCH project at Harvard is grateful for partial support from NSF grants AST-0407380, AST-0909073, and AST-1313370.

REFERENCES

Bellm, E. C., & Sesar, B. 2016, pyraf-dbsp: Reduction pipeline for the Palomar Double Beam Spectrograph, ascl:1602.002

Bellm, E. C., Kulkarni, S. R., Graham, M. J., et al. 2019, PASP, 131, 018002

Ben-Ami, S., Konidaris, N., Quimby, R., et al. 2012, Proc. SPIE, 844686

Blagorodnova, N., Neill, J. D., Walters, R., et al. 2018, PASP, 130, 035003

Bookmyer, B. B. 1977, PASP, 89, 533

Chambers, K. C., Magnier, E. A., Metcalfe, N., et al. 2016, arXiv e-prints, arXiv:1612.05560

Cenko, S. B., Fox, D. B., Moon, D.-S., et al. 2006, PASP, 118, 1396

Cutri, R. M., Wright, E. L., Conrow, T., et al. 2012, Explanatory Supplement to the WISE All-Sky Data Release Product

Donati, J.-F., Semel, M., Carter, B. D., Rees, D. E., & Collier Cameron, A. 1997, MNRAS, 291, 658

Donati, J.-F., Jardine, M. M., Gregory, S. G., et al. 2007, MNRAS, 380, 1297

Geier, S., Heber, U., Edelmann, H., et al. 2013, A&A, 557, A122

Geier, S., Raddi, R., Gentile Fusillo, N. P., et al. 2019, A&A, 621, A38

Gaia Collaboration, Brown, A. G. A., Vallenari, A., et al. 2018, A&A, 616, A1

Graham, M. J., Kulkarni, S. R., Bellm, E. C., et al. 2019, PASP, 131, 078001

Green, G. M., Schlafly, E. F., Zucker, C., et al. 2019, arXiv e-prints, arXiv:1905.02734

Grindlay, J., Tang, S., Los, E., et al. 2012, New Horizons in Time Domain Astronomy, 29

Hambsch, F.-J. 2012, Journal of the American Association of Variable Star Observers (JAAVSO), 40, 1003

Hameury, J.-M., & Lasota, J.-P. 2014, A&A, 569, A48

Heinze, A. N., Tonry, J. L., Denneau, L., et al. 2018, AJ, 156, 241

Hessman, F. V., Robinson, E. L., Nather, R. E., et al. 1984, ApJ, 286, 747

Huang, P., 2019, PhD thesis, Graduate Institute of Astronomy, National Central University

Kaiser, N., Burgett, W., Chambers, K., et al. 2010, Proc. SPIE, 77330E

Kato, T. 2019, PASJ, 71, 20

Kim, K.-M., Jang, B.-H., Han, I., Jang, J. G., Sung, H. C., and Chun, M.-Y. 2002, Journal of the Korean Astronomical Society, 35, 221

Kimura, M., Osaki, Y., Kato, T., et al. 2020, PASJ, 72, 22

Kochanek, C. S., Shappee, B. J., Stanek, K. Z., et al. 2017, PASP, 129, 104502

Kukarkin, B. V., Kholopov, P. N., Pskovsky, Y. P., et al. 1971, General Catalogue of Variable Stars, 0

Kurucz, R. 1993, ATLAS9 Stellar Atmosphere Programs and 2 km/s grid. Kurucz CD-ROM No. 13. Cambridge, 13

Labadie-Bartz, J., Pepper, J., McSwain, M. V., et al. 2017, AJ, 153, 252

Lasker, B. M., Lattanzi, M. G., McLean, B. J., et al. 2008, AJ, 136, 735

Mainzer, A., Bauer, J., Grav, T., et al. 2011, ApJ, 731, 53

Manek, J. 1997, Information Bulletin on Variable Stars, 4476, 1

Masci, F. J., Laher, R. R., Rusholme, B., et al. 2019, PASP, 131, 018003

Mason, E., & Howell, S. B. 2016, A&A, 589, A106

Meinunger, L. 1980, Information Bulletin on Variable Stars, 1795, 1

Morrissey, P., Conrow, T., Barlow, T. A., et al. 2007, ApJS, 173, 682

Ngeow, C.-C., Lee, C.-D., Yu, P.-C., et al. 2019, Journal of Physics Conference Series, 012010

Ochsenbein, F., Bauer, P., & Marcout, J. 2000, A&AS, 143, 23

Oke, J. B., & Gunn, J. E. 1982, PASP, 94, 586

Pojmanski, G. 1997, AcA, 47, 467

Pojmanski, G. 2002, AcA, 52, 397

Pojmanski, G., Pilecki, B., & Szczygiel, D. 2005, AcA, 55, 275

Rigault, M., Neill, J. D., Blagorodnova, N., et al. 2019, A&A, 627, A115

Ritter, A., Ngeow, C. C., Konidaris, N., et al. 2014, Contributions of the Astronomical Observatory Skalnate Pleso, 43, 209

Rivinius, T., Carciofi, A. C., & Martayan, C. 2013, A&A Rv, 21, 69

Samus', N. N., Kazarovets, E. V., Durlevich, O. V., Kireeva, N. N., & Pastukhova, E. N. 2017, Astronomy Reports, 61, 80

Sato, S., Chieh Huang, P., Chen, W. P., et al. 2019, Research in Astronomy and Astrophysics, 19, 136

Schindewolf, M., Németh, P., Heber, U., et al. 2018, A&A, 620, A36

Schmidt, G. D., Elston, R., & Lupie, O. L. 1992, AJ, 104, 1563

Shappee, B. J., Prieto, J. L., Grupe, D., et al. 2014, ApJ, 788, 48

Sigut, T. A. A., & Patel, P. 2013, ApJ, 765, 41

Skrutskie, M. F., Cutri, R. M., Stiening, R., et al. 2006, AJ, 131, 1163

Stellingwerf, R. F. 1978, ApJ, 224, 953

STScI Development Team 2013, pysynphot: Synthetic photometry software package, ascl:1303.023

Szkody, P., Michalsky, J. J., & Stokes, G. M. 1982, PASP, 94, 137

Szkody, P., Albright, M., Linnell, A. P., et al. 2013, PASP, 125, 142

Wolf, C., Onken, C. A., Luvaul, L. C., et al. 2018, PASA, 35, e010

Yu, P.-C., Yu, C.-H., Lee, C.-D., et al. 2018, AJ, 155, 91

Yu, P.-C., Lin, C.-C., Lin, H.-W., et al. 2016, AJ, 151, 121

Yu, P. C., Lin, C. C., Chen, W. P., et al. 2015, AJ, 149, 43

Zacharias, N., Monet, D. G., Levine, S. E., et al. 2005, VizieR Online Data Catalog, I/297

Zacharias, N., Finch, C. T., Girard, T. M., et al. 2012, VizieR Online Data Catalog, I/322A